

Yasemin Manavbasi

NKCS DERIVED PEPTIDES AS NOVEL CANCER THERAPEUTICS

DISSERTATION

zur Erlangung des akademischen Grades einer
Doktorin der technischen Wissenschaften

eingereicht an der

Technischen Universität Graz

durchgeführt am

Institut für Biophysik und Nanosystemforschung
Österreichische Akademie der Wissenschaften

bei

Univ. Doz. Dipl.-Ing Dr. Karl Lohner

Graz, Dezember 2010

Hayat boyu aldığım her kararda yanımda olan ve desteğini
hep hissettiğim biricik anneme.

STATUTORY DECLARATION

I declare that I have authored this thesis independently, that I have not used other than the declared sources / resources, and that I have explicitly marked all material which has been quoted either literally or by content from the used sources.

.....

Date

.....

Signature

Acknowledgement

Foremost, I would like to express my gratitude to my supervisor Karl Lohner for providing me a supportive environment and make this work possible. I learned a lot from his patience, his analytic thinking and positive attitude.

I would like to thank IBN director Peter Laggner for impressive and inspiring conversations we had from time to time.

It is a great pleasure to thank my colleagues/friends Beate Boulgaropoulos, Florian Prossnigg, Fabian Schmid and Daniela Frascione for their support; -physically or mentally-, for their patience and for our information exchange in many levels and for sharing this valuable time with them. Thanks to Bahar Özden for being my best friend and for standing by me in good and bad times even though we were far from each other.

I thank to all other colleagues in IBN for this pleasant working atmosphere.

I also wish to thank all the collaborator colleagues of our EU-Biocontrol Network, whose names I could not mention here. The financial support of the Marie Curie Training Network Biocontrol is gratefully acknowledged.

And finally, I owe my loving gratitudes to my mother, my father and my brother.

Content

STATUTORY DECLARATION	v
Acknowledgement	vii
Content	ix
Abstract	xi
Glossary	xv
Chapter 1 Introduction	1
1.1 Features of Biological Membranes	1
1.1.1 Structure and Composition of Biological Membranes	1
1.1.2 Importance of Lipid Sidedness and PS Localization	2
1.1.3 Membrane Mimic Systems as Our First Line of Research	5
1.2 Host Defense Peptides	5
1.2.1 HDP as a Novel Anticancer Agent	6
1.2.2 Mechanisms of Membrane Disruption and Necessary Features of a Potent HDP	9
1.2.3 Cancer Cell Membrane Susceptibility to HDPs	10
1.2.4 Parameters Influencing HDP Activity	10
1.2.5 Non Membranolytic Modes of Action	12
1.3 NK-Lysin, NK-2 and NKCS	12
1.4 Prostate Cancer	13
Chapter 2 Results	17
2.1 N-Terminal Segment of NKCS Is Responsible for PS Affinity	17
2.2 Prostate Cancer Toxicity of NKCS	35
Chapter 3 Summary and Outlook	67
Chapter 4 Reference List	71
Chapter 5 Curriculum vitae	89

Abstract

Discovered and isolated on the basis of their antibacterial activity, host defense peptides (HDPs) have gained a wide interest as novel therapeutic drugs. They are produced as a part of innate immunity by almost all species of living organisms (Hancock and Lehrer, 1998). HDPs are cationic, mostly short peptide sequences. Their secondary structure and origin vary widely, and their mechanism(s) of action suggest that cytotoxicity exerted by most of these peptides includes membrane damage and not via a receptor mediated pathway. Recently there has been a focus on their cytotoxic activity against cancer cells. The electrostatic attraction between the negatively charged components of the cancer cell membrane and the positively charged HDP is believed to play a role in the selective disruption of the membrane. However, it is still not known why some peptides are toxic to cancer cells while some are not (Hoskin and Ramamoorthy, 2008). Moreover, structural determinants that make an HDP cancer specific are mainly unknown.

The 27 residue, cationic NK-2 peptide that corresponds to the core region of NK-lysin, was shown to bear anticancer activity which correlated to the amount of surface-exposed negatively charged phosphatidylserine on cancer cells (Schroder-Borm et al., 2005). Cystein to serine replacement led to the design of NKCS which augmented its antibacterial activity. However, so far no study was conducted on its anticancer activity. Likewise, little is known about the determinants of the selective activity of NKCS. It was suggested that the two amphipathic helical segments of this peptide which are connected by a hinge region are important for the antimicrobial activity of NKCS, as deduced from model membrane studies (Gofman et al., 2010). In order to shed light on structure-activity relationships, within this thesis the N- and C-terminal segment of NKCS and derivatives thereof were synthesized and characterized with respect to their selective anticancer capabilities.

In the first part of this thesis the parent peptide NKCS and the two helical segments were characterized in respect of secondary structure and interaction with membrane model systems. Liposomes containing the negatively charged phosphatidylserine were used to mimic cancer plasma cell membranes and phosphatidylcholine to mimic healthy plasma cell membranes. Thermodynamic and leakage experiments showed that the N-terminal segment which had a higher α -helical than the C-terminal segment exhibited effects similar to NKCS, while the C-terminal peptide was rather inactive.

In the second part of this thesis we extended these studies to the dimeric form of the two peptide segments including Monte Carlo simulations and *in vitro* experiments. Cytotoxicity of the newly generated peptides was tested on LNCaP prostate cancer cell line as well as NIH-3T3

fibroblasts as healthy control to unravel their selectivity. This study showed that dimerization of the segments only improved the activity of the N-terminal segment. This peptide was superior to NKCS in terms of anticancer activity which correlated with its helical content and amphipathicity. However, the fine tuning of the parameters which can potentiate the therapeutic potency of cationic peptides needs further investigation.

Glossary

aa	amino acid
ACP	anticancer peptide
ATP	adenosine triphosphate
CD	circular dichroism
Cer	ceramide
CMC	critical micelle concentration
DAG	diacylglycerol
DPC	dodecylphosphocholine
DPPC	dipalmitoyl-phosphatidylcholine
DPPS	dipalmitoyl-phosphatidylserine
DSC	differential scanning calorimetry
EPC	ethanolamine phosphorylceramide
FTIR	Fourier transform infrared spectroscopy
GalCer	galactosylceramide
GlcCer	glucosylceramide
GM3	glycosphingolipid
HDP	host defense peptide
IPC	inositol phosphorylceramide
LNCaP	lymph node carcinoma of the prostate
NIH-3T3	National Institute of Health, USA; primary mouse embryonic fibroblast cells that were cultured by the designated protocol, so-called '3T3 protocol'
NK-2	residues 39-65 of the NK-Lysin
NKCS	cystein to serine replacement of NK-2
NK-Lysin	peptide of cytotoxic T and natural killer cells
PA	phosphatidic acid

PC	phosphatidylcholine
PE	phosphatidylethanolamine
PI	phosphatidylinositol
PIP	phosphatidylinositol-4-monophosphate
PIP2	phosphatidylinositol-4,5-biphosphate
POPC	palmitoyl-oleoyl-phosphatidylcholine
POPS	palmitoyl-oleoyl-phosphatidylserine
PS	phosphatidylserine
RBC	red blood cells
SAPLIP	saposin like protein
SDS	sodium dodecyl sulfate
SM	sphingomyeline

Chapter 1

Introduction

The description of biological membranes at first, was nothing more than a two dimensional liquid bilayer in which proteins are dispersed randomly (Singer and Nicolson, 1972).

1.1 Features of Biological Membranes

The current view of plasma membranes has changed since Singer and Nicholson postulated their Fluid Mosaic Model in 1972. The concepts developed during the course of three decades brought us to an understanding of a biomembrane that has variable domains, variable thickness and higher protein occupancy than once believed (Engelman, 2005). As the lipid bilayer makes up the core structure of the cell membrane by creating a two-dimensional solvent, without a plasma membrane the cell could not maintain its integrity as a coordinated chemical system. It does not only confine miscellaneous reactions into different compartments, but also the membrane itself functions as an organelle, hosting thousands of different molecules whose functions are essential for life.

1.1.1 Structure and Composition of Biological Membranes

Biological membranes are composed of more than two hundred different lipid species (Myher et al., 1989). To list, glycerophospholipids, phosphosphingolipids, glycosphingolipids and sterols are the major classes which make up the lipid bilayer. Phosphatidylcholine (PC) that belongs to the family of glycerophospholipids is the major component of animal cell membranes. Beyond doubt the major role of lipids is to form the bilayer structure. However, based on the reason of lipids' striking variety, there is a growing awareness towards their miscellaneous roles which contribute to the diversity of living beings. To exemplify, a typical mammalian plasma membrane constitutes 20-25% cholesterol by mass of the total lipids making up the bilayer while inner mitochondrial membrane lacks it totally (Moran A.L et al., 1994). Additionally, another feature of these molecules which astonishingly contributes to intracellular heterogeneity is their physical state which was shown to differ from membrane to membrane within a single cell (Mamdouh et al., 1998). The fact that biological membranes are highly heterogeneous in composition as well as

function both varying within and between cells founds the basis of the implementation of membrane targeted molecules, in our case; host defense peptides.

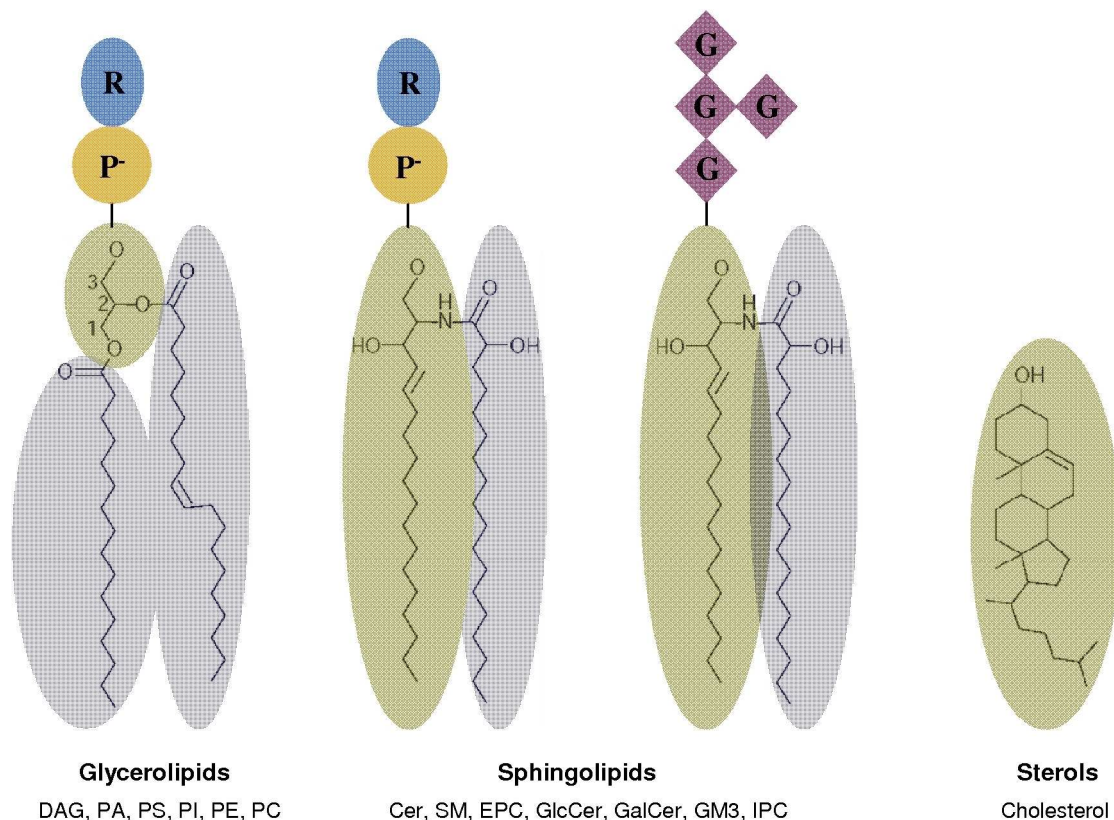


Figure 1 Three main classes of eukaryotic membrane lipids. **Glycerolipids:** They are based on glycerol (green shading) with two C16-C18 fatty acid chains (grey shading) which are linked at sn-1 and -2 forming diacylglycerol (DAG). The presence of a cis-double bond causes a kink in the acyl chain and decreases the packing density of the lipid. When a phosphate (P) is attached at sn-3 it forms phosphatidic acid (PA). This P can carry a head group (R) resulting in neutral (e.g. phosphatidylcholine (PC), phosphatidylethanolamine (PE)) or charged (e.g. phosphatidylserine (PS), phosphatidylinositol (PI)) lipids. **Sphingolipids** are based on a C18 sphingoid base (green shading) with amide linked to the nitrogen termed ceramide (Cer). The sphingolipid head group (R) can be phosphocholine (sphingomyelin (SM)) or phosphoethanolamine (ethanolaminephosphoryl ceramide (EPC)). In the case of glycosphingolipids, it can be glucose to form glucosylceramide (GlcCer) or galactose to produce galactosylceramide (GalCer), or there can appear additional monosaccharides (G) to form a wide array of glycosphingolipids (GM3). Phosphoinositol head group lead to inositolphosphorylceramide (IPC). **Sterols** are formed by planar four-ring structures such as cholesterol (Adapted from Holthuis and Levine, 2005).

1.1.2 Importance of Lipid Sidedness and PS Localization

Cellular membranes are composed of many more lipid species than a simple bilayer requires for its architecture which are known to be non-randomly shared between two leaflets. Membrane phospholipid asymmetry, the so called 'lipid sidedness' is an indispensable necessity of regular cellular function and homeostasis. There is indeed a unique pattern of lipid distribution matching the specific function of each cell type and inner subcellular organelles (Robert B. Genis, 1989). Furthermore many membrane bound enzymatic systems are dependent on a particular phospholipid composition. Choline containing phospholipids such as phosphatidylcholine (PC)

and sphingomyelin (SM) are located primarily in the extracellular facing leaflet, while aminophospholipids such as phosphatidylserine (PS) and phosphatidylethanolamine (PE) are found on the membrane's inner leaflet (Bruckheimer and Schroit, 1996). Other minor constituents such as phosphatidic acid (PA), phosphatidylinositol (PI), phosphatidylinositol-4-monophosphate (PIP) and phosphatidylinositol-4,5-bisphosphate (PIP₂) are also sequestered in the cytosolic side (Daleke, 2003). Considering these various lipid species, distinctive confinement of PS in the inner leaflet deserves a specific attention as it is a well-known characteristic of eukaryotic plasma membranes and therefore its exposure on the cell surface initiates substantial functional consequences (Bruckheimer and Schroit, 1996). As schematically represented in Figure 2, SM and PC show high outer leaflet distribution while PE is predominantly found in the inner leaflet and PS is completely confined to inner leaflet.

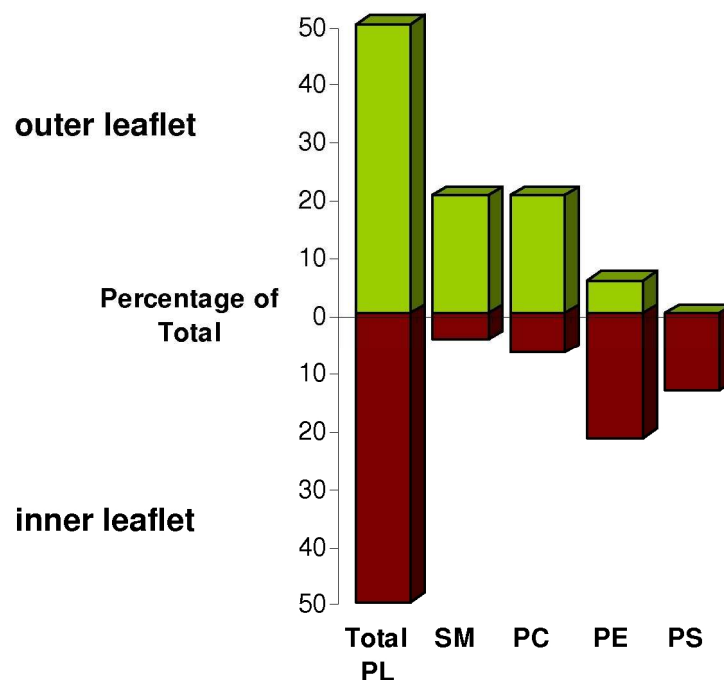


Figure 2 Representation of the relative distribution of the major phospholipids in human erythrocyte membrane. Phospholipid (PL), sphingomyelin (SM), phosphatidylcholine (PC), phosphatidylethanolamine (PE), phosphatidylserine (PS). (Adapted from Verkleij et al., 1973)

Transmembrane lipid asymmetry is generated by three classes of transporter proteins that are universal to most eukaryotic cells which are flippases, floppases and scramblases. The first class of transporters, aminophospholipid flippase, shows selectivity to PS and can be found in most plasma membranes. As shown in Figure 3, the aminophospholipid flippase (PS-translocase), transports PS into the inner layer, harvesting approximately one ATP for each molecule of lipid transported (Beleznay et al., 1993). Notably, enzyme's activity is inhibited by Ca⁺² which can be taken as an indication of PS exposure involvement in activated cells (Daleke and Huestis,

1985;Bitbol et al., 1987). The second class of ATP-dependent enzyme is exofacially-directed floppase, transferring PC and cholesterol to the outer leaflet. Compared to PS-translocase they work at a much slower rate. The third class of enzymes, scramblase, causes the passage of lipids bidirectionally and distributes phospholipids evenly between both membrane leaflets. They are stimulated by intracellular Ca^{2+} in activated cells and lead to rapid non-selective mixing (Bever et al., 1996).

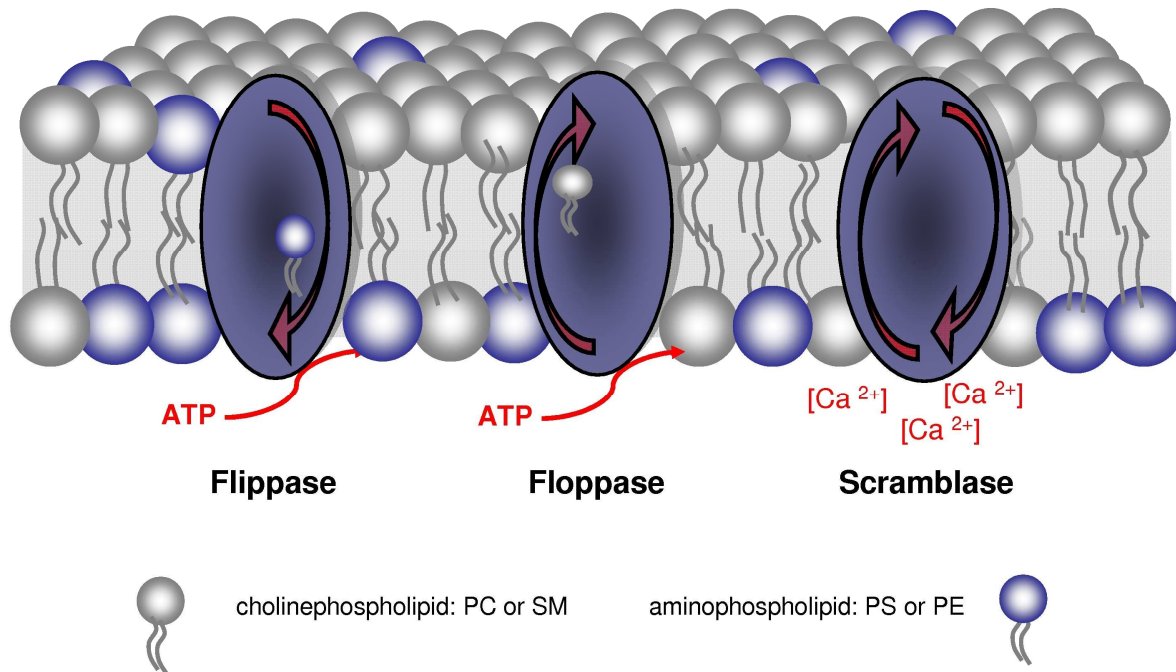


Figure 3 Exchange of lipids between two leaflets of membrane bilayer. ATP dependent uni-porters; **flippase** transports phosphatidylserine (PS) and phosphatidylethanolamine (PE) inwards while **floppase** transports phosphatidylcholine (PC) and sphingomyelin (Sph) outwards. Bidirectional transporter **scramblase** transports phospholipids randomly. Activation of scramblase occurs following a calcium influx $[\text{Ca}^{2+}]$ or on apoptosis signal. (Adapted from Zwaal et al., 2005)

Cells invest energy to these systems that are working in a concerted way to maintain a specific transmembrane phospholipid distribution. This is well evident for PS since its preservation in the inner leaflet has many important roles. Relocalization of PS in the outer leaflet however is known to be relevant to many physiological and pathological conditions, such as sickled red blood cells and their recognition by mononuclear phagocytes (Schwartz et al., 1985). Activated platelets also bear PS on their outer membranes as a result of high rate scramblase activity, which further initiates the blood coagulation cascade that guarantees effective blood coagulation (Bever and Williamson, 2010). However, undesired PS exposure on circulating blood cells carries the risk of thrombosis. On the contrary, impaired lipid scrambling manifests as a bleeding disorder, Scott Syndrome (Zwaal et al., 2004;Bever et al., 1983;Zwaal et al., 1977;Zwaal, 1978).

Furthermore exposure of PS on the surface of apoptotic cells is accepted as a hallmark of apoptosis which then triggers their specific recognition and clearance by macrophages (Fadok et al., 1992; Martin et al., 1995b). On the other hand, tumor cells also have shown to bear PS on their outer leaflets. Utsugi et al. has shown 3 to 7 times higher PS expression in the outer leaflet of tumorigenic cell lines compared to non-tumorigenic cell lines (Utsugi et al., 1991). The involvement of negatively charged amino phospholipid, PS in the outer leaflet matrix makes tumor cells slightly more negative compared to healthy cells which can be considered as a distinction threshold for a host defense peptide's selective killing activity (Papo and Shai, 2003b).

1.1.3 Membrane Mimic Systems as Our First Line of Research

Since living systems are highly complex and hard to mimic in total, it is conceivable to mimic the most prominent features of the biological systems as a first line of approach. There is no single experimental technique which allows understanding the whole process of the interaction between a host defense peptide (HDP) and a biological membrane. Due to this reason, we have to apply many biophysical techniques and integrate the information we gather to explain the process occurring during this interaction. A better understanding of HDP's activity on membranes can help us to design anticancer peptides with higher efficacy. The use of synthetic lipids together with peptides provides great advantages in the understanding of the effect of environmental factors, such as temperature, pH, ionic strength and hydration level on the interaction, while observing peptide conformational behavior and the dynamic properties of the lipid membrane. Undoubtedly, the self describing principal disparities between healthy mammalian cells and cancer cells are manifold as described in chapter 1.2.3, we concentrate our research on the charge difference them.

Since our research focuses on the exposure of PS on cancer cell membranes, we designed our experiments accordingly and used dipalmitoyl-phosphatidylserine (DPPS) or palmitoyl-oleoylphosphatidylserine (POPS) to estimate cancer selectivity of peptides. To unravel the activity and selectivity of the synthetic peptides we employed cell biology techniques using two different cell culture lines. Transferring biophysical data into *in vitro* experiments gives us a chance to observe the applicability of our expertise in biophysics into real life.

1.2 Host Defense Peptides

First emerged as antimicrobial peptides, host defense peptides have a wide variety of existence in nature. They are also called membrane active peptides and produced as a primary innate immune strategy by almost all species of living organisms (Hancock and Lehrer, 1998). HDPs are mostly short (15-60 amino acid residues) peptide sequences and active against bacteria, fungi, viruses and protozoa (Martin et al., 1995a). Ubiquitous existence of HDPs in animal and plant kingdom

suggests their important role in the evolution of complex multicellular organisms (Zasloff, 2002). In higher organisms they are mostly found on epithelial surfaces and phagocytic cells, where they are activated in response to bacterial infection (Papo and Shai, 2003a). HDPs are usually positively charged and mostly do not act via any specific receptor molecule on the cell membrane, instead they permeabilize or lyse the target membrane (Tossi et al., 2000; Zelezetsky and Tossi, 2006). The electrostatic interaction between the cationic peptide and the negatively charged components of bacterial cell membranes are believed to play an important role in selective killing of invading bacteria (Hoskin and Ramamoorthy, 2008). Their action rather stems from the unique property of their propensity of entering lipid environment with their hydrophobic side while being soluble in aqueous environment with their hydrophilic side (amphipathicity) (Izadpanah and Gallo, 2005). While HDPs can adopt α -helical, β -sheet, cyclic or loop structures (Lohner and Blondelle, 2005), they still share a set of common properties that highly effects their biological functions. Especially for the α -helical ones these properties can be listed as

- size,
- residue arrangement,
- charge (mainly cationic),
- charge distribution,
- degree of structuring,
- the overall hydrophobicity and,
- amphipathicity (distribution of polar and non-polar domains and the angles subtended by hydrophobic and hydrophilic faces)

These interrelated structural and physicochemical parameters determine their potency and selectivity (Zelezetsky and Tossi, 2006). That is why understanding and fine tuning of these parameters can help to improve development of new therapeutic agents.

1.2.1 HDP as a Novel Anticancer Agent

Besides their antibacterial activity, many HDPs are capable of killing a wide variety of cancer cells. Those that bear anticancer activity can be categorized as follows:

1. HDPs that are toxic against bacteria and cancer cells but not against normal mammalian cells, selective peptides.
2. HDPs that are non selectively killing bacteria, cancer cells and normal mammalian cells, (Hoskin and Ramamoorthy, 2008; Papo and Shai, 2005)

It is suggested that cytotoxic activity towards micro-organisms and cancer cells is a function of the cationicity and the secondary structure of HDPs (Leuschner and Hansel, 2004; Powers and Hancock, 2003). Elevated levels of negatively charged PS on the outer leaflet of cancer cells attract cationic peptides which is the basis for anticancer activity (Utsugi et al., 1991; Chen et al., 1997).

Electrostatic interaction favors binding of HDPs to the lipid membrane and further insertion of the peptide disrupts the packing of the phospholipid array. Thereby, permeability of the bilayer increases which results in necrotic killing of the tumor cell (Yang et al., 2004). Depending on the severity of the stress exerted by the peptide molecule, the process can lead to total breaking up of the cancer cell membrane architecture (Papo and Shai, 2005). While it is not known whether these two mechanisms, antibacterial and anticancer, are identical or different, it appears that designing an anticancer peptide is more challenging than designing an antimicrobial peptide, since transformed and non-transformed cells are more alike compared to differences between mammalian cells and bacteria (Shin et al., 2001).

Our immune system is programmed to recognize and eradicate cancer cells mainly via receptor mediated mechanisms (Dunn et al., 2002; Mocellin et al., 2004; Blattman and Greenberg, 2004). Under normal physiological conditions immune effectors can keep tumor growth under control. However, cancer cells have many ways to evade immune surveillance (Dunn et al., 2002). Unfortunately current conventional therapeutic approaches not only have many shortcomings in destroying pathological cells, but also they are causing many life quality diminishing side effects. In that regard, HDPs have many advantages over conventional cytotoxic chemotherapeutic agents which are discussed in detail in Chapter 1.4

An early study, conducted on magainin and its synthetic analogue against hematopoietic and solid tumors showed their cytolytic activity through channel formation. Moreover, cellular potential was found to be important for membrane disruption and cytotoxicity. Notably, replacement of D-aa has not changed the anticancer activity, which eliminates a receptor mediated pathway (Cruciani et al., 1991).

In 2005, the NK-lysin derivative peptide NK-2 was shown to kill cancer cells with increased surface PS (Schroder-Borm et al., 2005). The topic of this thesis focuses on further derivatives of NK-2, and proven anticancer activity of NK-2 is discussed in Chapter 1.3.

	Peptide	Primary aa sequence	Class	Net charge	Anticancer activity
Selective Peptides	NK-Lysin	GYFCESCRKIIQKLEDMVGPQPNEDTVTQAASQVCDKLKILR GLCKKIMRSFLRRISWDILTGKKPQAICVDIKICKE	α -helical	+6	Membranolytic (Andersson et al., 1995)
	NK-2	KILRGVCKKIMRTFLRRISKDILTGKK	α -helical	+9	Membranolytic; necrotic mechanism (Schroder-Born et al., 2005)
	NKCS	KILRGVSKKIMRTFLRRISKDILTGKK	α -helical	+9	Membranolytic (Gofman et al., 2010)
	Magainin II	GIGKFLHSAKFGKAFVGEIMNS	α -helical	+3	Membranolytic, channel formation (Cruciani et al., 1991)
	Lactoferricin B	FKCRRWQWRMKKLGAPSITCVRRAF	β -sheet	+8	Membranolytic (Eliassen et al., 2006), apoptosis inducer (Mader et al., 2005) Antiangiogenic (Mader et al., 2006)
Non-selective Peptides	Melittin	GIGAVLKVLTTGLPALISWIKRKRQQ	α -helical	+6	Membranolytic (Hristova et al., 2001) PLA2, PLD activator (Sharma, 1993;Saini et al., 1999)
	Tachyplesin I	KWCFRVCYRGICYRRCR	β -sheet	+6	Complement pathway mediated lysis, binds hyaluronan (Chen et al., 2005)
	LL-37	LLGDFFRKSKEKIGKEFKRIVQRIKDFLRNLPRTES	α -helical	+6	Membranolytic, toroidal pore (Henzler Wildman et al., 2003)
	HNP-1(β -defensin)	ACYCRIPACIAGERRYGTCTIYQGRLLWAFCC	β -sheet	+3	Membranolytic (McKeown et al., 2006;Lichtenstein, 1991) antiangiogenic (Chavakis et al., 2004)

Table 1 List of selective and non selective HDPs exhibiting anticancer activity.

1.2.2 Mechanisms of Membrane Disruption and Necessary Features of a Potent HDP

As mentioned above, the amphipathic nature of HDPs enables membrane permeabilization and/or perturbation. As shown in Figure 4 there are four models in discussion concerning the membrane lysis by HDPs. These are; barrel stave, torroidal pore, detergent like and carpet models. More than one model can be in use for a HDP's mode of action.

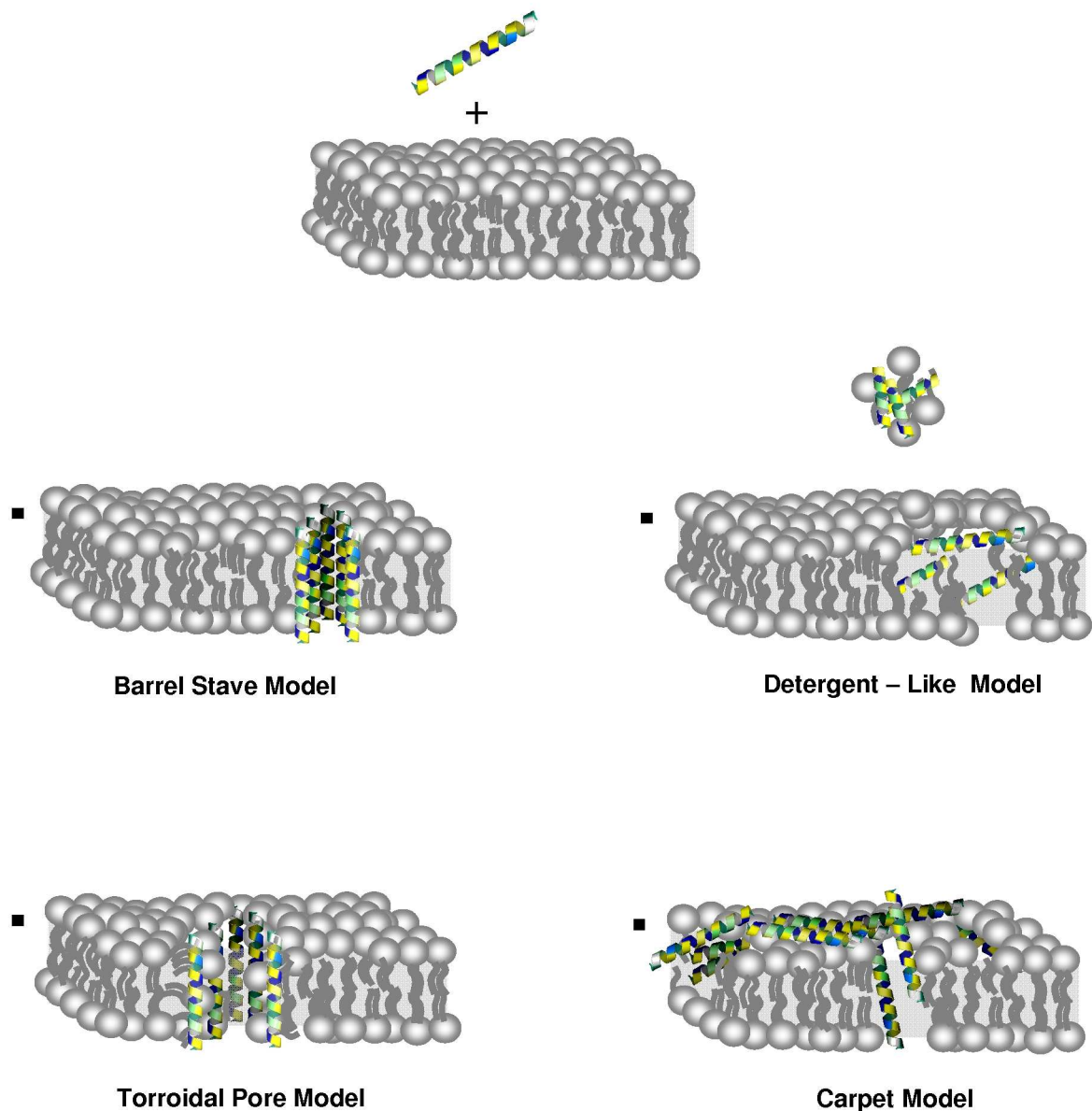


Figure 4 Cartoon illustrating different models of membrane permeabilization by host defense peptides. (Adapted from Papo and Shai, 2005; Hoskin and Ramamoorthy, 2008)

According to Shai, (Papo and Shai, 2005) cancer selective peptides that make up the first group bind to the membrane by electrostatic interactions and align parallel to the surface covering

it in a carpet like manner. After reaching a particular concentration, the peptides insert into the membrane and cause permeabilization or micellization. As an intermediate step transient pores can form. If the peptide is long enough to span the membrane, these pores are called toroidal pores and can lead to direct cell death (Ludtke et al., 1996; Matsuzaki et al., 1995). However, non selective peptides can bind via hydrophobic interactions and form the so called 'barrel-stave' kind of transmembrane pores (Ehrenstein and Lecar, 1977; Papo and Shai, 2005; Vogel et al., 1983).

Other models to mention are, the detergent like actions of linear amphipathic cationic antimicrobial peptides (Bechinger and Lohner, 2006), the sinking raft model (Pokorny and Almeida, 2004) and electroporation model (Miteva et al., 1999) which needs further investigation however it stands for a valuable tool to understand the mechanisms of certain HDPs.

The membranolytic action of HDPs is not confined to the cell membrane, some HDPs can transverse into cytosol and act on mitochondrial membrane causing swelling which then initiates apoptotic pathways (Mader et al., 2005). Likewise, there are other non-membranolytic modes of actions which are discussed in Chapter 1.2.5.

1.2.3 Cancer Cell Membrane Susceptibility to HDPs

There are fundamental differences between the cell membranes of malignant and non-malignant healthy cells. As mentioned above, PS exposure makes cancer cells slightly negative compared to healthy cells, however there are other molecules like o-glycosylated mucins contributing to the negative charge density on the outer leaflet (Utsugi et al., 1991; Yoon et al., 1996; Burdick et al., 1997). In addition, the cancer cell membrane is more fluid than its healthy counterpart which may enhance the lytic activity of HDP (Kozłowska et al., 1999; Sok et al., 1999). Furthermore, the existence of a high number of microvilli on their cell surface increases the overall contact area with HDPs (Domagala and Koss, 1980; Chaudhary and Munshi, 1995). On the other hand, cholesterol, the major sterol component of mammalian cell membranes (Simons and Ikonen, 2000) has been found to decrease the fluidity and thereby stabilize the integrity of the membrane. Notably, increased cholesterol limits the insertion of HDP which may be a protective mechanism for eukaryotic cells from the cytolytic effect of HDPs (Leuschner and Hansel, 2004). Taken together, these characteristics give rise to efficient killing of neoplastic cells by HDPs while sparing untransformed cells.

1.2.4 Parameters Influencing HDP Activity

In order to understand the determinants of effective toxicity of HDPs against cancer cells at lower concentrations than required to kill healthy mammalian cells, the structural basis for cancer cell membrane specificity must be elucidated. The interaction of HDPs with lipid membranes

involves a number of steps, which include initial binding through a mixture of hydrophobic and electrostatic interactions, induction of secondary structure following the binding, re-orientation, insertion, and finally further partitioning of the peptide into the membrane (White and Wimley, 1998). Considering these steps, some criteria have been studied to shed light on the variables that fine tune the process. First of all quantitative structure function correlation studies show the necessity of a lateral amphiphilic structure which is actually a common architectural motif and manifested also in the structure of naturally occurring transmembrane proteins. Studies which are mostly concentrated on α -helical proteins indicate the necessity of a well segregated polar/charged residues on one side creating a polar sector and hydrophobic residues accumulated on the other side, forming the hydrophobic sector. Together with the angle of the cationic sector, the sector depth, that is characterized by amino acid side chains, influences the HDP's potency and spectrum of activity (Zelezetsky and Tossi, 2006). For an effective membrane insertion, helical structuring is required in order to secure the above mentioned sectors well defined and functional along the helix. For this reason the presence of α -helical stabilizing aminoacids, such as alanine, (Lyu et al., 1991) is important in the ability to adopt an active α -helical conformation. As a result of a study done in 2004, an optimized antitumor peptide is described as a 14aa long peptide having a net positive charge of 7. It has been suggested that amphipathic α -helical conformation is more important for antitumor activity compared to antimicrobial activity (Yang et al., 2004). Besides of these peptide-only properties, ionic strength and pH of the milieu are expected to influence the conformation that peptide adopt and accordingly affect their interaction to cell membranes (Blondelle et al., 1999). Yet, tumor microenvironment is known to be acidic (De Milito and Fais, 2005) which can play a role in peptide secondary structure. Other structural parameters coming from the membrane side, such as hydrocarbon chain length of lipids and the membrane curvature are also of great importance (Edited by Karl Lohner, 2001).

While the secondary structures vary between peptide classes, above mentioned common features mainly determine the effect. Parameters stemming from the peptide lipid interaction can be listed as follows and together with other properties they determine the pattern of the lytic effect.

- The structural folding in membranes; secondary structure, dynamics and orientation
- Oligomerization (oligomeric state)
- Peptide concentration
- Membrane composition

In consideration of a potential therapeutic application, all these information must be taken into account to optimize an anticancer peptide with an improved efficacy and selectivity.

1.2.5 Non Membranolytic Modes of Action

Apart from cell membrane lytic mode of action, there is growing evidence that alternative mechanisms exist. As mentioned previously, HDPs can induce swelling of mitochondria and cause release of cytochrome c. Released cytochrome c initiates the Apaf-1 oligomerization and caspase 9 activation which can further lead to many of the hallmarks of apoptotic symptoms (Cory and Adams, 1998). In addition to the mitochondrial pathway, some HDPs can induce apoptosis via receptor mediated pathway or both (Chen et al., 2001).

Melittin can be given as an example for a different pathway which has an affinity towards ras oncogen expressed cells and selectively destroys them by hyperactivating phospholipase A₂. Moreover alleferons have shown to have immunomodulatory properties stimulating natural killer lymphocytes (Chernysh et al., 2002).

1.3 NK-Lysin, NK-2 and NKCS

NK-Lysin belongs to the 8-9 kDa, saposin-like family of proteins which are called SAPLIPs, sharing a common alpha-helical fold with a conserved half-cystein pattern. While they are structurally conserved, their functions divers widely (Munford et al., 1995; Liepinsh et al., 1997; Anderson et al., 2003). These proteins are stored in respective cellular cytotoxic granules and are secreted in contact with a victim cell (Schroder-Borm et al., 2003). NK-Lysin is described as the effector molecule of cytotoxic T and NK cells which are, along with neutrophils and macrophages, the primary effector cells of innate immune system (Andersson et al., 1995). Andersson et al. isolated NK-Lysin from porcine intestinal tissue due to its antibacterial activity and lytic activity against NK sensitive murine tumour cell line. NK-Lysin is the porcine counterpart of human granulysin (Pena et al., 1997). In order to improve membrane selectivity, NK-2, a 27-residue peptide, representing the third and the fourth helices (residues, 39-65) of NK-Lysin has designed. NK-2 is effective against clinical isolates of *Candida albicans*, broad spectrum of bacteria (Andra and Leippe, 1999), protozoan parasite *Trypanosoma cruzi* (Jacobs et al., 2003) and more importantly cancer cells (Schroder-Borm et al., 2005), and it shows low toxicity towards human cells (Jacobs et al., 2003; Andra and Leippe, 1999). Characterized by strong binding preference, anticancer activity of NK-2 showed a good correlation with cancer cells with increased surface PS amount (Schroder-Borm et al., 2005). Cystein to serine residue replacement of NK-2 gave rise to the peptide NKCS, which is a more potent peptide in terms of antibacterial activity (Gofman et al., 2010).

1.4 Prostate Cancer

Altered cell physiology can give rise to more than 100 cancer types, still they share six common traits as listed below (Hanahan and Weinberg, 2000);

1. They respond to even very weak growth signals which are ignored by healthy cells or they produce their own growth signals.
2. They do not respond to anti-growth signals.
3. Acquired capability of escaping from programmed cell death; resistance to apoptosis.
4. They have limitless replication ability.
5. Sustained capacity of new blood vessel generation; angiogenesis.
6. Ability to escape from tumor mass and evade new body parts; metastasis.

Accumulated rich and complex body of knowledge on cancer so far have led to the determination of these features listed which help scientists to think of new treatment regimes. Clear enough, this is a tough work which necessitates a holistic approach of genetics, histopathology, biochemistry, immunology pharmacology and biophysics. In 2000 Hanahan postulated that cancer biology and treatment would become a science with a conceptual structure and logical coherence that rivals that of chemistry or physics. Based on the progress in cancer biology and biotechnology new means of treatments are being introduced to markets perpetually. However this disease remains as one of the biggest problems of human health, mainly because of the development of resistance to each agent applied or severe side effects due to non-specific drug actions. To exemplify, radiotherapy, chemotherapy, surgery or the combination of these three are included in the generally practiced modalities of treatment, unfortunately causing well documented severe complications such as; necrotic bones, skin ulcers, damage to the spinal cord, to cardiac muscle, and to lung tissue (Udagawa, 2009). Therefore new agents with new mode of action have an invaluable place in cancer therapy.

According to American Prostate Cancer Foundation, in every 2,5 minutes a new case is diagnosed and unfortunately one of them dies in every 19 minutes. It is considered as the most common non-skin cancer in America. Treatments for prostate cancer include surgery (Schaeffer et al., 2010), chemotherapy, radiotherapy, (Schutz and Oh, 2010), and hormone deprivation therapy (Choong and Basaria, 2010). Recently, new experimental therapies have also been explored, such as targeted gene therapy (Lu, 2009) and immunotherapy (Drake, 2010). Even though modalities of therapy are manifold, cancer cells have different escape mechanisms for each agent applied. To list shortly, conventional chemotherapeutic agents that typically act only on rapidly dividing cells lack specificity and as mentioned above, they damage normally functioning tissues intensely (Cassidy and Misset, 2002;Kalyanaraman et al., 2002). Moreover, cancer cells in slow proliferation phase can escape from chemotherapeutic drugs that act on DNA

synthesis levels (Naumov et al., 2003). Furthermore increased expression of drug detoxifying enzymes and drug transporters which keep the drug away from its target renders the cancer cell resistant to chemotherapy. Besides, cancer cells can also increase their ability to repair DNA damage and continue growing (Gatti and Zunino, 2005). Provided these facts, formulation of a targeted drug sparing healthy tissues will always remain as a main interest of cancer research. Given this negative charge marking on cell membranes as a unique property of many cancer cell types it would be quite an appropriate link to develop anticancer therapeutics based on PS exposure phenomenon which should bring in many advantages over conventional cytotoxic drugs. Since the proposed killing mechanism is the disruption of the cell membrane, they are not expected to induce resistance in cancer cells. Moreover, HDPs are able to kill multidrug resistant cancer cells as well (Lapis, 2010).

It is expected that biophysical studies focusing on mechanisms of membrane disruption regarding dynamics, topology and the role of membrane and peptide elements in the interaction will unravel the rationalization of a well documented selectivity and activity of each peptide practised and as a result will help to formulate an anticancer peptide with an applicable efficacy.

Chapter 2

Results

In the following chapter I present two papers; first one being 'N-terminal Segment of NKCS Is Responsible for PS Affinity' and the second one being 'Prostate Cancer Toxicity of NKCS'.

2.1 N-terminal Segment of NKCS Is Responsible for PS Affinity

Yasemin Manavbasi, Agnieszka Rzeszutek*, Regine Willumeit*, Karl Lohner

Institute of Biophysics and Nanosystems Research, Austrian Academy of Sciences, Graz, Austria

* GKSS-Research Center, Geesthacht, Germany

Keywords: NKCS, phosphatidylserine, host defense peptides, anticancer peptides

Abbreviations

PS phosphatidylserine, PC phosphatidylcholine, HDPs host defense peptides, NK-2 residues 39-65 of NK-lysin, NKCS cysteine to serine replacement of NK-2, DPPC 1,2-dipalmitoyl-*sn*-glycero-3-phosphocholine, DPPE 1,2-dipalmitoyl-*sn*-glycero-3-phospho-L-serine, POPC 1-palmitoyl-2-oleoyl-*sn*-glycero-3-phosphocholine, POPS 1-palmitoyl-2-oleoyl-*sn*-glycero-3-phospho-L-serine, DSC differential scanning calorimetry, CD circular dichroism, CMC critical micelle concentration, SDS sodium dodecyl sulfate, DPC dodecylphosphocholine, PBS phosphate buffer saline, HEPES N-2-hydroxyethylpiperazine-N'-2-ethanesulfonic acid, ANTS 8-aminonaphthalene-1,3,6-trisulfonate, DPX p-xylene-bis-pyridinium bromide, LUVs large unilamellar vesicles, Q net charge, *H* hydrophobic ratio, μ hydrophobic moment.

Abstract

The NK-lysin derived cationic peptide NK-2 composed of two helices connected by a hinge region was shown to have antimicrobial and anticancer activity. Cystein to serine replacement, termed NKCS, did not affect the structure of the peptide which was supposed to play a crucial role in its antibacterial activity. However, no study focusing on its importance in anticancer activity has been described so far. Thus, we synthesized the N- and C-terminal segment (NK-14, NK-15) and characterized the parent peptide NKCS as well as the two segments in respect of secondary structure and interaction with membrane model systems.

It has been shown that cancer cells expose negatively charged phosphatidylserine (PS) on the outer leaflet of their plasma cell membrane. In order to unravel the specific interaction of the peptides liposomes containing dipalmitoyl- or 1-palmitoyl-2-oleoyl-phosphatidylserine (DPPS or POPS respectively) were used to mimic cancer plasma cell membranes and dipalmitoyl- or 1-palmitoyl-2-oleoyl-phosphatidylcholine (DPPC or POPC) vesicles to mimic healthy plasma cell membranes.

Calorimetric experiments showed that the cationic peptides exhibited a higher affinity to anionic PS, whereby the degree of perturbation of the bilayer varied within the peptides studied being most prominent for NKCS and NK-14. The phase behavior of phosphatidylcholine (PC) was negligibly affected by all peptides which correlated with the absence or minor hemolytic activity of the peptides observed only at high peptide concentrations. Leakage experiments gave more detailed information on the specific interaction of the N- and C-terminal segment, respectively. Latter induced no marked release of entrapped fluorophore even at a lipid-to-peptide molar ratio of 6:1, where full rupture was observed for the parent peptide and NK-14. Shuffling of the amino acid sequence as well as exchange of the anionic Glu by the cationic Lys within the C-terminal segment did not alter the properties of NK-15. Circular dichroism spectra showed that all the peptides exhibited an unordered structure in aqueous environment, but adopted to different degrees secondary structures in the presence of sodium dodecyl sulfate (SDS) and dodecylphosphocholine (DPC) micelles as membrane mimetic environments. Thereby, NKCS and NK-14 showed the highest amount of α -helical content which can be correlated with their higher membrane activity suggesting that the N-terminal segment is responsible for selective activity.

Introduction

Cancer is a group of diseases characterized by uncontrolled growth and spread of aberrant cells and it remains as one of the biggest health problems threatening human health and life quality. Despite of the advances in cancer biology and biotechnology it is likely that every newly introduced therapy regime evokes its own side effects (Udagawa, 2009). Complexity of cancer and its well documented diverse properties lead scientists into two different ways of thinking. One approach uses the dissection of the phenomenon and complex nature of cancer which results in focusing on diversity and therefore treating each cancer type differently. On the other hand we propose a unifying approach by taking a common phenomenon in various cancer types as a starting point and hit the pathology “from the bull’s eye”, the negatively charged exposed phosphatidylserine (PS). Its exposure on the outer membrane leaflet of the plasma membrane of cancer cells results in a fundamental difference between healthy and cancer cell membranes, (Utsugi et al., 1991; Papo et al., 2003; Papo and Shai, 2003b). As a result cancer cells carry a net negative charge which differentiates them from their healthy counterparts.

Discovered and isolated on the basis of their antibacterial activity, some host defense peptides (HDPs) are known to kill cancer cells. In nature HDPs act within the primary innate immune strategy in almost all species of living organisms (Hancock and Lehrer, 1998). They are mostly short peptide sequences with cationic properties exhibiting various secondary structures. While some HDPs are non-selective, some spare healthy cells and show selective activity in killing cancer cells mostly by the destabilization of the cytoplasmic membrane. Their selective killing ability is widely believed to stem from their affinity towards correspondent membranes composed of particular lipids, such as the above mentioned PS (Hoskin and Ramamoorthy, 2008). Thereby, HDPs are capable of differentiating cancer cell membranes from healthy cell counterparts and cause lysis on the former by specific interaction with PS. The precise process of killing and the determinants of the mechanisms are still a matter of debate, however, proposed mechanisms include membrane lysis and perturbation of the membrane structure (Papo and Shai, 2005). The improvement of a refined peptide with a high efficacy towards cancer cell membranes is within the scope of this research.

NK-2 peptide corresponds to the 3rd and the 4th helices of the NK-lysin, a porcine homolog of human granulysin, which is considered as a promising candidate for clinical applications (Pena et al., 1997). Principally, NK-2 was designed to enhance its antimicrobial activity compared to the NK-lysin (Schroder-Borm et al., 2003). Later on it has been shown that this 27-residue peptide, NK-2, selectively causes necrotic killing on various cell lines which expose negatively charged PS on their surfaces, such as, some neuroblastoma and leukemia cell lines (Schroder-Borm et al., 2005). Replacement of the cysteine residue with a serine residue led to the synthesis of NKCS which enhanced its antibacterial activity (Andra et al., 2007). It is

known that the two helices are connected by a hinge region. However, so far the exact role of each helix on its antibacterial or anticancer activity has not been elucidated (Gofman et al., 2010; Schroder-Borm et al., 2003). To understand the effect of each helix and to gain insight into the structure-function relationship we synthesized the individual helices separately and tested the newly derived peptides against cancer and healthy cell membrane mimic systems.

In that regard we used differential scanning calorimetry (DSC) to estimate the affinity of derivatives towards two different lipid matrixes (PS and phosphatidylcholine (PC), mimicking cancer and healthy mammalian cell membranes, respectively). Leakage assay was conducted to investigate their potency to perturb bilayer integrity. Furthermore, circular dichroism (CD) measurements were performed to correlate the biophysical data to the secondary structures of the peptides. Finally the hemolytic activity on red blood cells was tested to determine the non-selective derivatives of the newly synthesized peptides.

We have shown that the N-terminal segment is responsible for PS affinity of NKCS and thus it is reasonable to pursue this newly synthesized peptide to design an active and selective anticancer agent.

Materials and Methods

Calculation of Peptide Parameters

The net charge (Q) of each peptide was calculated by subtracting the one aspartic acid residue, when it exists, from the sum of all positive charges arising from the lysine and arginine residues plus adding one positive net charge owing to the C-terminal amidation. The hydrophobic moment (μ) was calculated according to the algorithm presented by Zidovetzki et al. (Zidovetzki et al., 2003). The total hydrophobic ratio (H) was calculated from the antimicrobial peptide database (Wang and Wang, 2004).

Preparation of Liposomes

Appropriate amounts of the phospholipid stock solutions were dried under a stream of nitrogen and stored in vacuum overnight to remove the organic solvent completely. Then the dried lipid films were hydrated with phosphate buffered saline (PBS, 20 mM, 130 mM NaCl, pH 7.4) in the presence or absence of peptides at a temperature above the gel to liquid-crystalline phase transition of the respective phospholipid under periodical vigorous vortex mixing.

Circular Dichroism

Measurements were performed at room temperature on a Jasco J 715 Spectropolarimeter (Jasco, Gross-Umstadt, Germany). Far UV-CD spectra were recorded at a lipid-to-peptide molar ratio of 25:1 using quartz cuvettes with an optical path length of 0.02 cm. The CD was measured between 260 and 180 nm with a 0.2 nm step resolution. Each spectrum is the average of three scans to improve the accuracy. 4 mg/ml stock solutions of peptides were dissolved in 10 mM Hepes buffer and the spectra were recorded at the presence of 20 mM sodium dodecyl sulfate (SDS) and 20 mM dodecylphosphocholine (DPC) to mimic some of the characteristics of cancer and healthy mammalian membranes. Respective backgrounds for each experiment were subtracted during the measurement. Percentage of the secondary structures were calculated by Dichroweb, CDSSR Convolution Program using reference set 4 (Whitmore and Wallace, 2004; Whitmore and Wallace, 2008).

Differential Scanning Calorimetry

Differential scanning calorimetry (DSC) studies were performed with 2-dipalmitoyl-*sn*-glycero-3-phospho-L-serine (DPPS) and 1,2-dipalmitoyl-*sn*-glycero-3-phosphocholine (DPPC) lipids with the Microcal VP-DSC high-sensitivity differential scanning calorimeter (Microcal, Northampton, MA, USA). Individual experiments were repeated three times for the sample reproducibility, the second heating scan was taken for data analysis and representation. Scans were covering a range of 15 degrees above and 20 degrees below the main transition temperature. All heating and cooling scans were recorded at a constant rate of 30°C/h. Pre-scan thermostating was set to 10 minutes for the heating scans and to 1 minute for the cooling scans to reach thermodynamic equilibrium. The total lipid concentration used for the DSC scans was 1 mg/ml. Data acquisition and analysis were done using Microcal Origin software (Microcal). Calorimetric enthalpies were calculated by integrating the peak areas after baseline adjustment and normalization to the mass of phospholipid. The phase transition temperature was defined as the temperature at the peak maximum.

Leakage of ANTS/DPX

Leakage of aqueous contents from liposomes was determined using the ANTS/DPX assay (Ellens et al., 1985a). As a first approximation for cancer cell membrane negatively charged 1-palmitoyl-2-oleoyl-*sn*-glycero-3-phospho-L-serine (POPS) was used. As a healthy cell membrane mimic 1-palmitoyl-2-oleoyl-*sn*-glycero-3-phosphocholine (POPC) was used lipid films were hydrated with a buffer containing 12.5 mM ANTS, 45 mM DPX, 68 mM NaCl and 10 mM Hepes at pH 7.4 as described above for DSC measurements. Liposomal dispersions were extruded (Mini Extruder, Avanti Polar Lipids Inc. Alabaster, Alabama, USA) at least 21 times through a polycarbonate

filter of 0.1 μM pore size at a temperature above their transition temperature to acquire uniform large unilamellar vesicles (LUVs). In order to separate unencapsulated free ANTS/DPX from the ANTS/DPX containing vesicles by exclusion chromatography, a separation column filled with SephadexTM G-75 was used. The phospholipid concentration was determined by phosphorus analysis so that peptide to lipid ratios in the measuring cuvette can be calculated. Fluorescence spectroscopy measurements were performed on a SPEX FluoroMax-3 Spectrofluorimeter (HORIBA Jobin-Yvon, Longjumeau, France) combined with Datamax software. Fluorescence intensity was observed at 37°C under constant stirring. Excitation and emission monochromators were set to 360 nm and 530 nm, respectively. Measurements were performed in a buffer containing 10 mM Hepes, 140 mM NaCl and 1 mM EDTA at pH 7.4. LUVs were added to the cuvette to achieve a final lipid concentration of 50 μM . Fluorescence emission was recorded as a function of time before and after the addition of incremental amounts of peptide to give a final concentration of 8.3 μM . The maximum level of fluorescence, determined by the lysis of the liposomes with Triton X-100, was assigned as 100% leakage.

Hemolysis

The hemolytic activity of the peptides was determined using human erythrocytes (group 0 rhesus positive) which were used within two days after collection. Firstly, heparinized blood was centrifuged for three minutes at 2000 rpm then the supernatant was discarded and the pellet was washed with pH 7.4 PBS. The derived erythrocyte pellet was subsequently diluted with MES buffer (20 mM morpholinoethanesulfonic acid, 140 mM NaCl, pH 5.5) until 20 μL of this suspension added to 980 μL of double distilled water had the optical density of 1.4 at a wavelength of 412 nm. This value corresponds to 5×10^8 cells per ml. Equally, the peptides were diluted in MES buffer to the desired concentrations before 20 μL of the erythrocyte suspension was added to 80 μL of peptide solution. As a control 20 μL of erythrocyte suspension was mixed with 80 μL of double distilled water, resulting 100% lysis of the erythrocytes. The negative control was made by mixing 20 μL of erythrocyte suspension and 80 μL of MES buffer where the lysis is zero. Thereafter, the suspensions were incubated for 30 minutes at 37°C. Directly after incubation the samples were stored on ice and 900 μL MES buffer was added. All suspensions were centrifuged for ten minutes at 2000 rpm to sediment all intact erythrocytes. Finally, the absorbance was measured with a spectrometer (Tecan, Crailsheim, Germany) at 412 nm wavelength.

Design of NKCS Derivatives

The development of new anticancer peptides based on the NKCS sequence stemmed from the fact that NKCS is composed of two helices connected by a hinge. The first step was to understand

the individual affinities of the two helices towards cancer mimic membranes and further to understand if the activity of NKCS depends on any of these helices alone. Due to this reason NK-14 and NK-15 were synthesized corresponding to the N and C terminal part, respectively. Then, the negatively charged D in the C-terminal sequence was exchanged with positively charged K, termed NK-15-dk, and finally we scrambled the amino acids of that part to compare the activity with the original C-terminal part and named the peptide NK-15-s.

Results

Conformational Investigations

To gain knowledge on the activity-structure relationship of the NKCS and the newly derived peptides, the conformation of the peptides was investigated by CD spectroscopy. Spectra were recorded at 25:1 surfactant-to-peptide molar ratio. In order to observe the conformational state changes of the peptides upon addition of 20 mM SDS and DPC micelles, respectively, initially, spectra of the peptides in water were recorded.

At this concentration both surfactants are above their critical micellar concentration. Micelles formed by SDS are used as a simple mimetic of negatively charged bilayers. As reviewed in Blondelle et al. (Blondelle et al., 1999) above its CMC, SDS has been reported to be a stabilizer of alpha helical conformations and therefore one should consider each peptide's helical tendency with respect to each other.

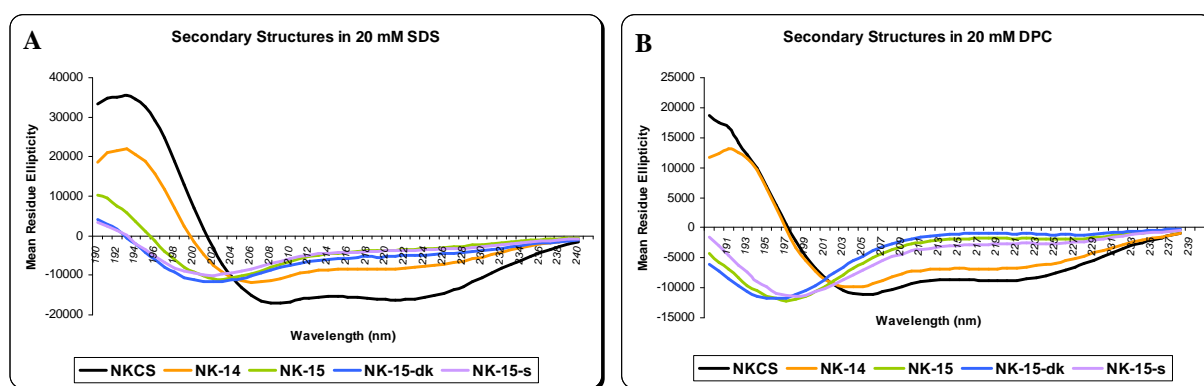


Figure 1 Circular dichroism spectra of NKCS and derived peptides in the presence of 20 mM SDS (A) and 20 mM DPC (B). Spectra recorded at a surfactant-to-peptide molar ratio of 25:1.

The CD spectrum of NKCS and all derivatives in water is characterized by a negative peak at around 198 nm and a positive peak around 215 nm, which is an indication of random coil arrangement (data not shown). As it is shown in Figure 1A, upon addition of SDS NKCS exhibits two minima at about 209 nm and 222 nm and a maximum at about 194 nm, which is consistent

with the presence of a α -helical conformation. The NK-14 spectrum showed the same property with the minima slightly shifted to lower wavelength. Dichroweb convolution (Whitmore and Wallace, 2004) also showed that NKCS has the highest helical content (59%) which is followed by NK-14 (35%). NK-14 has a higher content of beta structure as compared to NKCS (20% and 9%, respectively). Spectra gathered from NK-15, NK-15-dk and NK-15-s in the presence of SDS showed the same features with a negative peak at around 201 nm and a positive peak at 190 nm. According to Dichroweb convolution program, these three peptides have the lowest α -helical (13%) and highest random coil propensity (34%) amongst all the peptides tested (Table 1).

The same set of experiments was performed in the presence of DPC micelles (Figure 1B). The spectrum of NKCS and NK-14 then showed two negative peaks at around 206 nm and 222 nm and one positive peak at around 192 nm, which are again indications of α -helical content. However, according to Dichroweb convolution program, helical contents are lower as compared to SDS micelle environment (31 % and 30 % respectively). On the otherhand, NK-15, NK-15-dk and NK-15-s showed a negative peak at around 197 nm which is a strong indication of random coil arrangement. As a result, considering C-terminal peptides, amino acid distribution did not affect the secondary structure.

	% alpha		% beta		% turn		% random coil	
	SDS	DPC	SDS	DPC	SDS	DPC	SDS	DPC
NKCS	59	31	9	19	13	20	20	29
NK-14	35	30	20	22	20	20	25	27
NK-15-27	13	6	30	33	23	25	34	36
NK-15-27-dk	13	6	29	32	25	26	34	35
NK-15-27-s	13	9	27	30	26	25	34	36

Table 1 Secondary structure of NKCS and derived peptides in cancer cell membrane mimic (SDS) and healthy mammalian cell membrane mimic (DPC) environments at a surfactant-to-peptide molar ratio of 25:1.

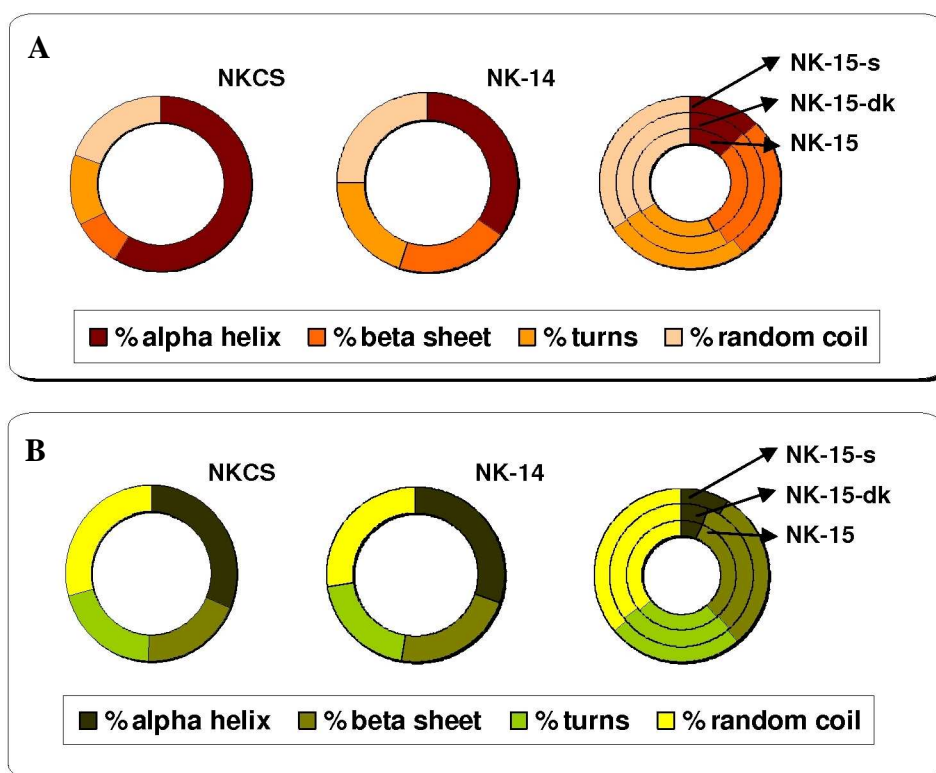


Figure 2 Percentage representation of α -helical, β -sheet, β -turn and random coil structures of NKCS and derived peptides in the presence of SDS (A) and DPC micelles (B) at a surfactant-to-peptide molar ratio of 25:1

Figure 2 gives another representation of the amount of secondary structure of the N-terminal and C-terminal peptides compared to the parent peptide NKCS at a surfactant-to-peptide molar ratio of 25:1, which was also used for leakage and calorimetric experiments.

Leakage of ANTS/DPX

Measuring the release of fluorescence dye ANTS induced by the addition of peptides from lipid vesicles allowed to determine the effect of peptides on the bilayer integrity of POPC and POPS. Peptides were checked for their ability to cause leakage on these two different lipid systems, POPS as cancer cell membrane mimic and POPC as healthy cell membrane mimic. We started with the molar ratio of lipid-to-peptide of 25:1 and went down to approximately 6:1 by adding peptides cumulatively.

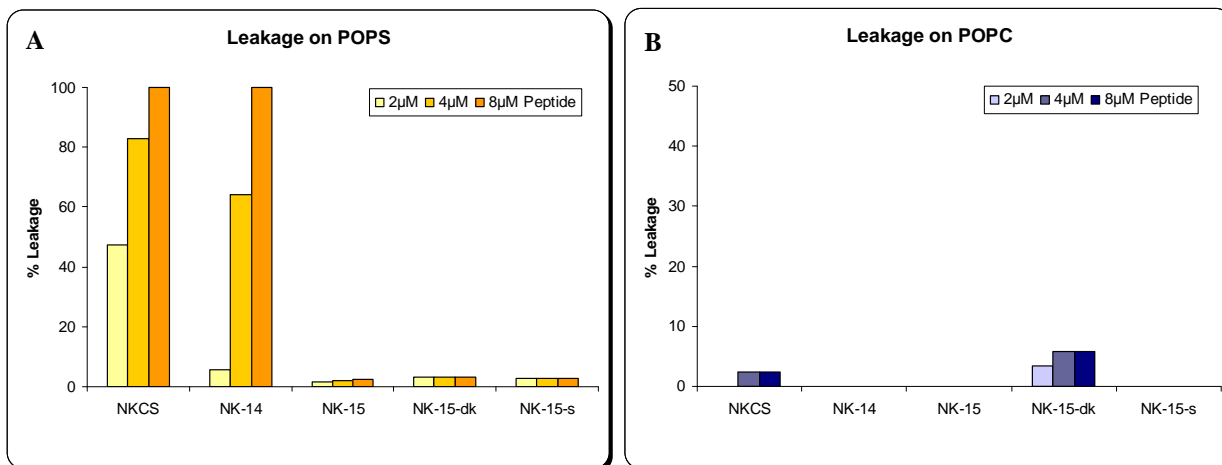


Figure 3 Leakage caused by cumulative addition of peptides to liposomes composed of POPS (A) and POPC (B). Data show the effect of 2, 4 and 8 μ M peptide corresponding to 25:1, 12:1 and 6:1 lipid-to-peptide molar ratio, respectively.

As shown in Figure 3A, only NKCS and NK-14 caused 100% leakage at a lipid-to-peptide molar ratio of 6:1. NKCS is still more potent than its N-terminal part inducing a significant leakage already at the lowest concentration used. The C-terminal peptide derivatives caused negligible leakage at all concentrations. On POPC liposomes (Figure 3B) only NK-15–dk and NKCS caused minor leakage at all concentrations.

Differential Scanning Calorimetry

The thermotropic phase behavior of pure DPPS lipid has a characteristic gel to liquid crystalline phase transition temperature of 52,6 $^{\circ}$ C with a little shoulder on the liquid crystalline side which can be seen in Figure 4A being in agreement with earlier data (Sevcsik et al., 2008).

The thermograms of DPPS liposomes recorded in the presence of NKCS differ significantly from the one of pure DPPS. Both the transition enthalpy and the transition temperature decreased. Moreover we observed a splitting of the main transition. As a result, the thermodynamic parameters of the first transition and the main transition were calculated separately and can be found in Table 2. Moreover, the shape of the main transition indicated overlapping transitions, which however could not be deconvoluted into individual transitions. The large width of the transitions indicates a loss of cooperativity, i.e. the presence of smaller lipid domains undergoing the phase transition. Upon addition of NK-14 we also observed a broadening of the endothermic heat capacity curve with a strong tailing towards the low temperature side. Again, similar to the presence of NKCS, overlapping transitions can be deduced from the shape of the thermogram. However, the change in total enthalpy was not as prominent as in the case of NKCS.

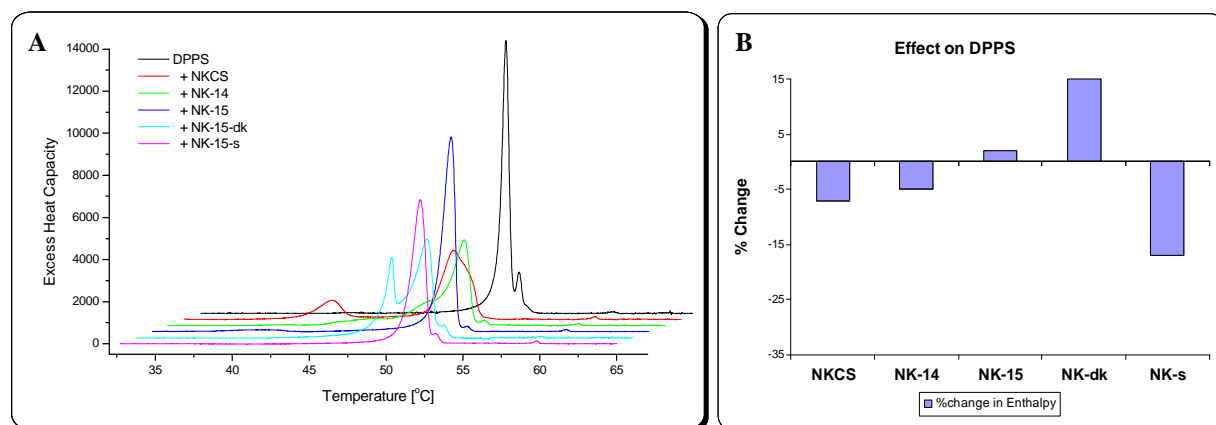


Figure 4 DSC thermograms of DPPS in the absence and presence of NKCS and derivatives at a lipid-to-peptide molar ratio of 25:1 (A). Change in total enthalpy in the presence of NKCS and derivatives (B).

While the addition of NK-15 did not provoke any prominent effect on the thermodynamic parameters of DPPS, NK-15-dk caused almost a 15% increase in the transition enthalpy. More strikingly, in the presence of this peptide a splitting of the main transition and shift of both transitions to lower temperature was observed. Upon addition of NK-15-s, the main transition enthalpy decreased. However, the main transition temperature was affected to a less degree.

	DPPS					
	T_1 (°C)	ΔH_1 (kcal/mol)	$\Delta T_{1/2}$ (°C)	T_m (°C)	ΔH_m (kcal/mol)	$\Delta T_{1/2}$ (°C)
pure	n.a.	n.a.	n.a.	52,6	10,0	0,5
+NKCS	42,3	1,9	1,8	50,2	7,4	2,2
+NK-14	47,3	1,2	3,6	51,9	8,3	1,35
+NK-15	n.a.	n.a.	n.a.	52,1	10,2	0,9
+NK-15-dk	49,3	4,1	0,7	51,6	7,6	1,4
+NK-15-s	n.a.	n.a.	n.a.	52,2	8,3	1,00

Table 2 Thermodynamic parameters of DPPS in the absence and presence of NKCS and derivatives at a lipid-to-peptide molar ratio of 25:1. T_1 (°C), transition temperature of peptide-enriched domain, T_m (°C), main transition temperature and their respective enthalpy (ΔH_1 , ΔH_m), and transition half-width ($\Delta T_{1/2}$ and $\Delta T_{1/2}$).

The heat capacity curve obtained for pure DPPC is consistent with the previously published data (Zweytick et al., 2006) which is characterized by two phase transitions, the first one being the pre-transition from the lamellar-gel ($L_{\beta'}$) to the ripple-phase ($P_{\beta'}$) at 35°C, the

second one, main or chain melting transition, from the ripple phase to the fluid phase (L_α) at 41,7°C. Table 3 shows the corresponding thermodynamic parameters.

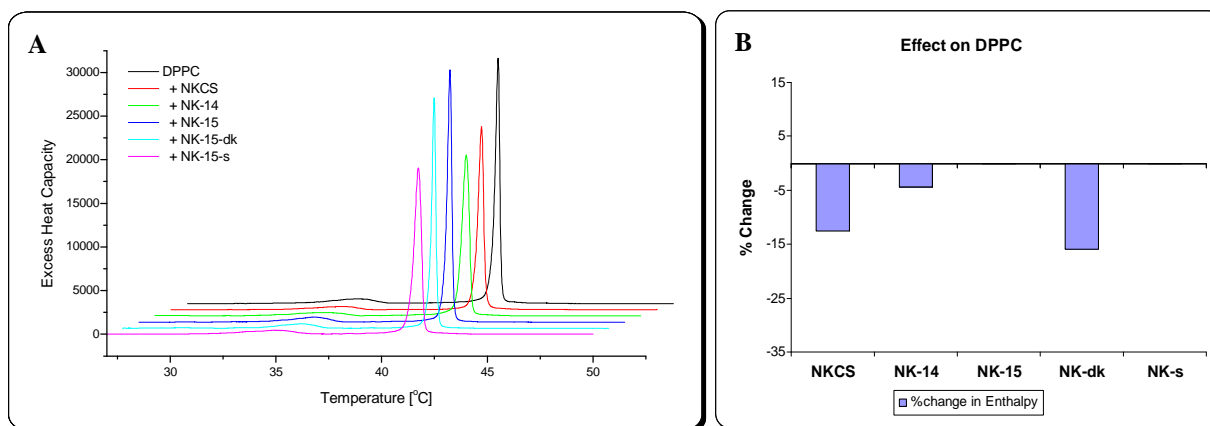


Figure 5 DSC thermograms of DPPC in the absence and presence of NKCS and derivatives at a lipid-to-peptide molar ratio of 25:1 (A). Change in main transition enthalpy in the presence of NKCS and derivatives (B).

Figure 5A shows the heating scans of DPPC in the absence and presence of peptides. While the chain melting temperature was not affected in the presence of any peptides, some affected the main transition enthalpy (Figure 5B). NKCS and NK-15–dk decreased it by 15% and in the presence of NK-14 the enthalpy decreased by 6%. NK-15 and NK-15-s have no significant effect on DPPC liposomes. NK-14 and NK-15-s broadened the main transition which indicates a decrease of its cooperativity. Finally, none of the peptides had a remarkable effect on the pre-transition, which is very sensitive to incorporation of additives.

	DPPC					
	T_{pre} (°C)	ΔH_{pre} (kcal/mol)	$\Delta T_{pre/2}$ (°C)	T_m (°C)	ΔH_m (kcal/mol)	$\Delta T_{1/2}$ (°C)
pure	35,1	1,2	2,4	41,7	8,8	0,25
+NKCS	35,7	0,9	2,35	41,7	7,7	0,30
+NK-14	35,0	1,0	2,8	41,7	8,4	0,40
+NK-15	35,3	1,2	2,0	41,7	8,8	0,24
+NK-15-dk	35,5	1,0	2,0	41,7	7,4	0,23
+NK-15-s	34,9	1,1	2,75	41,7	8,8	0,39

Table 3 Thermodynamic parameters of DPPC in the absence and presence of NKCS and derivatives at a lipid-to-peptide molar ratio of 25:1. Pre- and main transition temperature (T_{pre} , T_m), pre and main transition enthalpy (ΔH_{pre} , ΔH_m) and respective transition half width ($\Delta T_{pre/2}$, $\Delta T_{1/2}$).

Hemolysis

To study the selectivity, the peptides were tested against human erythrocytes. The lysis at concentrations of 1, 10 and 100 μM is displayed in Figure 6. None of the peptides induced noteworthy hemolysis. It is remarkable that the N-terminal segment did not induce any significant hemolysis even at the highest concentration used. This is in contrast to NKCS and the C-terminal peptides, which induced some hemolysis at this concentration.

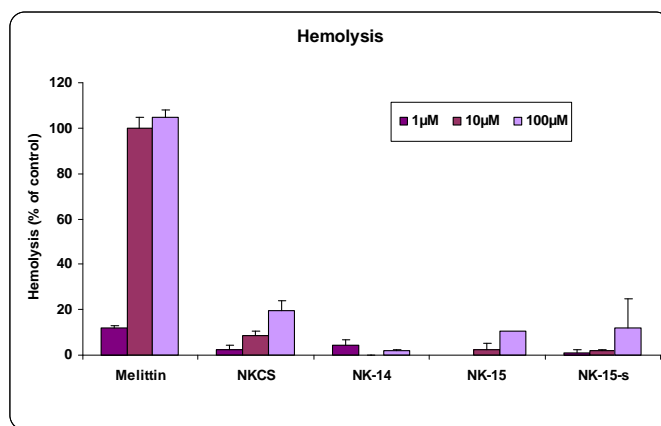


Figure 6 Hemolytic activity of NKCS and derivatives at three different peptide concentrations against human erythrocytes in comparison with melittin as a positive control. Concentration of cells: 5×10^8 cells/ml.

Discussion

In order to get a better understanding of the mechanism of anticancer peptides, which supposedly act at the membrane level (Mader and Hoskin, 2006), a number of membrane mimetic studies have been performed. This work focusses on the cationic NKCS belonging to the category of HDPs. Taking PS exposure as the main difference between cancer and healthy mammalian cell membranes (Utsugi et al., 1991; Yang et al., 2004) we studied the structure-activity relationship of NKCS and derived peptides using PS lipid systems. To evaluate their specificity we tested the peptides using PC lipid systems and performed hemolytic assays.

So far, it is not possible to predict the activity of a peptide just by knowing its amino acid sequence. Moreover, most peptides without disulfide bridges simply adopt random coil structure in water and fold into their secondary structures only in the proximity of a membrane or a hydrophobic environment (Bello et al., 1982). NKCS was reported to adopt two α -helices in the presence of lipidic environment which are separated by a hinge region. Thus, in the present study four new cationic peptides (Table 4) were designed on the basis of the double helical structure of NKCS in order to unravel the elements of NKCS's activity, i.e. to dissect possible specific involvement of the N- or C-terminal segment.

Peptide	Sequence	n	Q	μ	H	% helicity		100% leakage of PS	% hemolysis of 100 μ M
						SDS	DPC		
NKCS	KILRGVSKKIMRTFLRRISKDILTGKK	27	+10	5,12	37%	59	31	8 μ M	20
NK-14	KILRGVSKKIMRTF	14	+6	4,92	42%	35	30	8 μ M	2
NK-15	LRRISKDILTGKK	13	+5	3,21	30%	13	6	-	10
NK-15-dk	LRRISKILTGKK	13	+7	3,18	30%	13	6	-	n.a.
NK-15-s	LRGISKKIDRTLK	13	+5	4,79	30%	13	6	-	12

Table 4 Sequence and physicochemical parameters of NKCS and derived peptides (length (n), net charge (Q), hydrophobic moment (μ), total hydrophobic ratio (H)), α -helical content in SDS and in DPC micellar environment, as well as leakage and hemolytic activity.

Since the electrostatic interaction between the negatively charged PS head group of phospholipid and a cationic peptide starts the process of membrane interaction, it is not surprising that the charge is an important factor determining an HDP's activity (Yang et al., 2004). However, one should note that this interaction which initially favors binding of the peptide to the membrane surface is not sufficient to cause disruption of a membrane (Blondelle et al., 1999). With a net charge of +10, NKCS is the most cationic peptide we have investigated showing the greatest activity towards POPS liposomes. The distribution of the cationic residues of NKCS follows a distinct pattern, if plotted on a helical wheel projection (Figure 7). This presentation also gives an indication of the amphipathicity of the peptide when it is structured into an ideal α -helix. For the ease of understanding, the cationic sector is marked by a red angle and the arrow in the center stands for the direction of the hydrophobic moment which is different for each peptide. A well defined cationic sector (polar sector) is important for peptide's activity (Zelezetsky and Tossi, 2006). A distinct cationic sector can also be deduced for the NKCS derived peptides as shown in Figure 7. It is important to keep in mind that the wheel projection is not the real structure of the peptides, but depicts the relative distribution of the charged and the hydrophobic amino acids along an ideal helix.

The activity of NKCS was followed by NK-14 which is a 14 amino acid peptide with a net charge of +6. Its amino acid distribution along the helix also reflects a well defined separation between the polar and non-polar residues (Figure 7). Interestingly, the cationic sector of NK-14 is relatively narrow as compared to NKCS and displays a larger hydrophobic face, which may result in a deeper penetration of this peptide. In the presence of these two peptides we observed the same tendency on the thermodynamic properties of the lipids which indicated a loss of chain correlation and destabilization of the gel phase. The shorter NK-14 is almost as active as the parent peptide on POPS, the cancer cell membrane mimic.

NK-15, the C-terminal segment of the parent peptide, has a similar length as NK-14 and a net charge of +5. However, this peptide exhibits a smaller hydrophobic face on a putative helical structure indicating reduced amphipathicity. In accordance with this observation, it showed no activity on POPS liposomes. Furthermore, in the presence of this peptide the thermodynamic properties of DPPS were affected only slightly. DK replacement of the C-terminal peptide (NK-15-dk), leading to a net charge of +7 but not affecting the amino acid distribution, i.e. its amphipathicity, did not improve the activity on POPS liposomes. On the contrary, it decreased the selectivity causing leakage on POPC system as also observed for NKCS. Furthermore, both peptides decreased the transition enthalpy dramatically on DPPC lipid system which is also reflected in the hemolytic activity of NKCS. Thus we can conclude that exchanging the negatively charged D with a positively charged K decreased the selectivity of the peptide and did not result in any gain towards POPS affinity.

Scrambling of the amino acids of the C-terminal segment in a way that the peptide displayed a more confined cationic sector as well as a broader hydrophobic face than NK-15 did not result in higher activity.

Peptides with high hydrophobic moments, which is a quantitative expression of amphipathicity (Eisenberg et al., 1982), show increased membrane permeabilizing activity at PC rich membranes (Wieprecht et al., 1997). This is in agreement with the leakage and thermodynamic data obtained in the presence of NKCS which has the highest μ value among the peptides studied. Thus the capability of the hydrophobic moment to finetune membrane activity suggests that hydrophobic interactions play a more important role than electrostatic peptide-lipid interactions (Wieprecht et al., 1997). Basic properties like the threshold hydrophobicity are definitely important in HDPs activity (Yang et al., 2002). In general, high μ values correlated with the destabilizing effect on bilayers of NKCS derived peptides. Considering NKCS and both terminal segments, we observed increased leakage of POPS with the higher amount of helical percentage. It is also important to note that neither scrambling of the amino acid sequence nor the dk replacement affects the degree of structuring. According to our results, helicity together with a high hydrophobic moment is indispensable for PS selectivity of an HDP. Further systematic studies may reveal a threshold for each of these variables, beyond which a peptide seems to lose its selectivity.

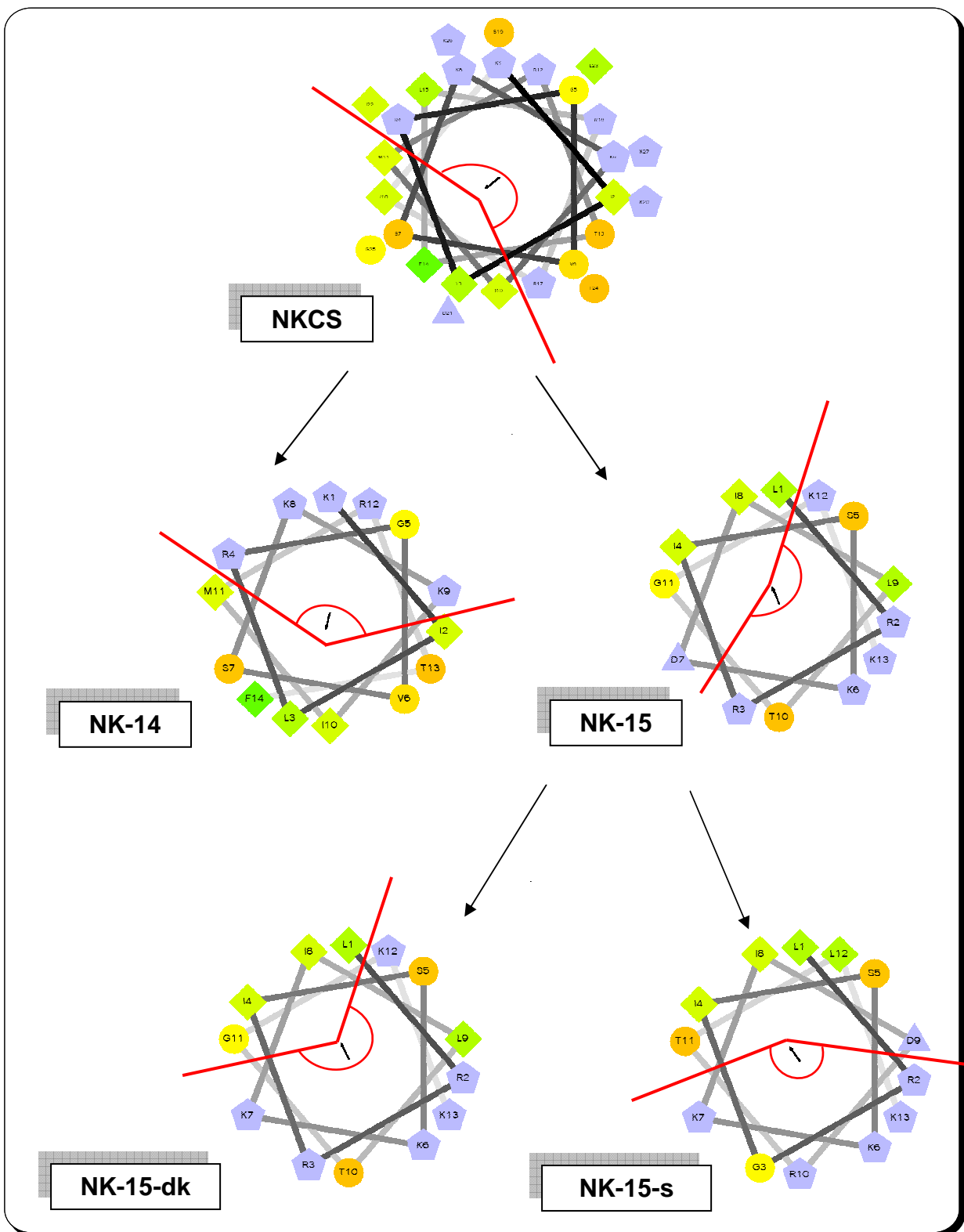


Figure 7 Schematic sketch of the development of NKCS derived peptides together with their helical wheel representations. Format code: Circles are hydrophilic, diamonds are hydrophobic, triangles are potentially negatively charged and pentagons are potentially positively charged residues. Color code: Zero hydrophobicity is yellow, the amount of hydrophobicity increases as the green color increases. Hydrophilic residues are red and the amount of red decreases as the hydrophilicity decreases. Potentially charged residues are light blue. Arrows indicate the angle of the hydrophobic moment (Zidovetzki et al., 2003). The cationic sector is marked by a red line.

2.2 Prostate Cancer Toxicity of NKCS

Yasemin Manavbasi, Yana Gofman*, Nir Ben-Tal*, Regine Willumeit[#], Karl Lohner

Institute of Biophysics and Nanosystems Research, Austrian Academy of Sciences, Graz, Austria

* Department of Biochemistry, Tel Aviv University, Israel

[#] GKSS-Research Center, Geesthacht, Germany

Key Words: anticancer peptides, amphiphatic peptides, helicity, phosphatidylserine, membrane mimics,

Abbreviations

PS phosphatidylserine, PC phosphatidylcholine, HDPs host defense peptides, NK-2 residues 39-65 of NK-lysin, NKCS cystein to serine replacement of NK-2, LNCaP lymph node carcinoma of the prostate, NIH-3T3 National Institute of Health, USA; primary mouse embryonic fibroblast cells that were cultured by the designated protocol, so-called '3T3 protocol', RBC red blood cells, Q net charge, *H* hydrophobic ratio, μ hydrophobic moment, DPPC 1,2-dipalmitoyl-*sn*-glycero-3-phosphocholine, DPPS 1,2-dipalmitoyl-*sn*-glycero-3-phospho-L-serine, POPC 1-palmitoyl-2-oleoyl-*sn*-glycero-3-phosphocholine, POPS 1-palmitoyl-2-oleoyl-*sn*-glycero-3-phospho-L-serine, DSC differential scanning calorimetry, CD circular dichroism, CMC critical micelle concentration, SDS sodium dodecyl sulfate, DPC dodecylphosphocholine, PBS phosphate buffer saline, Hepes N-2-hydroxyethylpiperazine-N'-2-ethanesulfonic acid, ANTS 8-aminonaphthalene-1,3,6-trisulfonate, DPX p-xylene-bis-pyridinium bromide, LUVs large unilamellar vesicles, PI propidium iodide, ACP anticancer peptides, MC Monte Carlo.

Abstract

Host defense peptides (HDPs) which were initially isolated due to their antibacterial activity, have been shown to exert toxic effect on cancer cells (Hoskin and Ramamoorthy, 2008). These peptides can discriminate between different membranes due to their intrinsic properties. It has been shown that, owing to the exposed anionic lipid, phosphatidylserine (PS) which normally resides in the inner leaflet of mammalian plasma cell membrane, the outer membrane leaflet of a cancer cell is slightly more negative than its healthy counterpart (Papo and Shai, 2005). Thus we investigated HDPs to elucidate the necessary features to selectively kill PS exposed cells. NKCS (Cys-Ser replacement), derived from NK-lysin, is known for its high antibacterial activity (Gofman et al., 2010) and there are studies regarding the anticancer activity of its precursor NK-2 showing necrotic killing on cancer lines which bear PS on their outer membrane leaflet (Schroder-Borm et al., 2005). It is known that NKCS like NK-2 is composed of two helices connected by a hinge region. Our former study showed the importance of the N-terminal segment on its PS selectivity. Therefore, we extended these studies to the dimeric form of the N- and C-terminal peptide segments as it was reported that peptide size is an important parameter for anticancer activity and compared their behavior to their parent peptide NKCS.

The secondary structure of the peptides was determined by circular dichroism (CD) spectroscopy and Monte Carlo (MC) simulations showing that the peptides are unstructured in water. Both approaches showed that in cancer membrane mimetic environment a significant α -helical content was only found for NKCS and the N-terminal peptides being most pronounced for the dimeric form of the N-terminal segment (NK-14-2) which resulted in a highly amphipathic structure. Monte Carlo simulation revealed that this peptide had the strongest binding energy to PS containing membranes. Furthermore, the simulation showed that only NKCS and NK-14-2 significantly insert into the lipid bilayer. These findings correlate with observations from calorimetric and leakage experiments showing that NK-14-2 was most effective in perturbing bilayer structure and in inducing leakage. While no leakage was induced by the monomeric form of the C-terminal segment, the dimer showed release of entrapped fluorophore from the vesicles at high peptide concentrations.

Cytotoxicity of the newly generated peptides was tested on LNCaP (lymph node carcinoma of the prostate) as well as NIH-3T3 fibroblasts as healthy control to unravel their selectivity. Our results show that dimerization of the segments only improved the activity of the N-terminal segment. This peptide was even superior to NKCS in terms of anticancer activity which correlated with its helical content and amphipathicity. However, the fine tuning of the parameters which can potentiate the therapeutic potency of cationic peptides needs further investigation

Introduction

Cancer, the uncontrolled growth of malignant cells, is a major health problem of modern medicine and second most common cause of death in the United States. Each and every type of therapy is associated with its own potential risks. Due to the fact that all neo-plastic agents have serious side effects, a novel therapy is indispensable. Cationic host defense peptides (HDPs), initially discovered due to their antimicrobial activity, are mostly small amino acid sequences and bear amphipathic structure upon membrane interaction. HDPs are a group of molecules endowed with activity to a very broad spectrum of microorganisms. These naturally occurring HDPs have been found in every species that has been investigated from fungi to animals. For an up to date list see the website <http://aps.unmc.edu/AP/main.php>. It has been shown that while some HDPs show non selective toxicity, some HDPs are active against only human pathogens or cancer cells. Accordingly, knowledge of precise structure activity relationship of HDPs is required for promising areas of research in therapy and medicinal chemistry. The structure and activity of HPDs have been subject to several reviews (Hoskin and Ramamoorthy, 2008;Papo and Shai, 2005;Papo and Shai, 2005).

Unlike healthy cells, some cancer types expose phosphatidylserine (PS) on their outer membrane. This negatively charged lipid serves as a marker on the surface which then initiates the binding of the HDP and further killing of the aforementioned cell (Papo et al., 2006;Schroder-Borm et al., 2005) . However, the exact mechanism of action is still on debate. Upon interaction with a particular cytoplasmic membrane, in our case cancer cell membrane, HDP adopts its active secondary structure. Mostly they exhibit amphipathicity which can be described as a cylinder with one face composed of non-polar amino acids and the other face composed of polar amino acids. So far it is known that both the cationicity and the hydrophobicity of the peptides are important for the initial attraction to the cancer cell membrane. Intercalation of the peptide is then enabled by hydrophobic interactions between the lipid acyl chains and the hydrophobic helix region of the peptide. It is thought that these cationic and amphiphilic peptides act by a direct impact on the cancer cell membrane, therefore it is anticipated that no resistance against the HDPs will occur.

To favor HDPs exploitation as anticancer drugs, it is indispensable to determine their exact mode of action together with the variables leading to their selective activity. HDPs originate from miscellaneous sources and can adopt various secondary structures. There is no positional conservation of even classes of amino acids in their sequences. Even though the relevance of the different parameters that determine the structure-activity relationship have been evaluated by using a sequence template guide, the outcome has arisen as a list of parameters rather than a rule defining the relationship (Zelezetsky and Tossi, 2006). Due to these reasons, it seems not feasible to predict their activity just by doing systematic research. On the other hand,

by creating synthetic peptide libraries based on a naturally occurring HDP, it is possible to gain insight into the mechanism of action and eventually improve anticancer activity and cell selectivity. Such an approach was shown to be effective for their antimicrobial activity (Hancock and Chapple, 1999).

NKCS which is a derivative of NK-2 peptide is known for its strong antibacterial activity (Gofman et al., 2010). There are studies about anticancer activity of its precursor NK-2, where it has been shown that NK-2 causes necrotic killing on cancer lines which bear PS on their outer membrane leaflet (Schroder-Borm et al., 2005). NKCS is known to consist of two helices connected by a hinge region. Our former study has shown the importance of the N-terminal helix on its PS selectivity.

Yang et al. (Yang et al., 2004) reported a strong correlation between antitumor activity and a net positive charge, peptide length and the ability to adopt an amphipathic α -helical conformation. In order to reach a conclusion for the NKCS peptide duplicates of C and N-terminal segment were investigated by the help of biophysical methods, modeling and *in vitro* assays. Additionally, construction of duplicates enables to observe the mass effect. Correlation of the experimental data with the physicochemical properties of the peptide unravels indispensable variables for potent anticancer activity.

To reveal the secondary structure of peptides circular dichroism (CD) studies were performed and correlated with data from Monte Carlo (MC) simulations. Latter also gave information concerning their membrane binding energy, insertion and location in bilayer model systems. The propensity to perturb the integrity of such bilayers was assayed by leakage and thermodynamic experiments. The cytotoxic activity of the peptides was investigated on prostate cancer cell line LNCaP (lymph-node carcinoma of the prostate). The specificity of peptides was determined by measuring the toxicity against murine originated 3T3-NIH fibroblast cells and human red blood cells (RBC).

We demonstrated that in biophysical studies, the newly derived NK-14-2, the dimeric form of NK-14, showed high affinity towards PS which correlated well with *in vitro* studies, where this peptide exerted high toxicity towards this cancer cell line which exposes PS on their outer membrane leaflet.

Materials and Methods

Peptides

NKCS and derivatives were synthesized by NeoMPS, Inc. (San Diego, CA, USA) in a purity grade > 96% as determined by RP-HPLC performed by the manufacturer. The sequences can be

seen in Table 1. All peptides were synthesized with an amidated C-terminus. Melittin, used as a control peptide for hemolytic and cytotoxicity assays was purchased from Sigma-Aldrich (Munich Germany) with approx. 70% purity. All peptides were dissolved either in phosphate buffered saline (PBS, 20mM Napi, 130mM NaCl, pH 7.4) or in water depending on the experimental conditions at a concentration of 3 mg/ml and stored at -20°C.

Calculation of Peptide Parameters

The net charge (Q) of the each peptide was calculated by subtracting the one aspartic acid residue, when it exists, from the sum of all positive charges arising from the lysine and arginine residues plus adding one positive net charge owing to the C-terminal amidation. Total hydrophobic ratio (H) was obtained from antimicrobial peptide database (Wang and Wang, 2004). Hydrophobic moment (μ) was calculated according to the algorithm presented by Zidovetzki et al. (Zidovetzki et al., 2003).

Design of NKCS Derivatives

Our aim to develop new antitumor peptides based on the NKCS sequence stemmed from the fact that NKCS is composed of two helices connected by a hinge region. As it is clearly shown in the first part of this thesis, initially we investigate the individual affinities of the two helices towards cancer mimic membranes. Now on the basis of data reported in literature and the results we gathered, we hypothesized that duplication of each part should increase their activity. Therefore we designed NK-14-2, which is the duplication of N-terminal peptide, and NK-15-2, which stands for the duplication of the C-terminal peptide.

Preparation of Liposomes

Appropriate amounts of the phospholipid stock solutions were dried under a stream of nitrogen and stored in vacuum overnight to remove the organic solvent completely. Then the dried lipid films were hydrated with PBS (20mM Napi, 130mM NaCl, pH 7.4) at a temperature above the gel to liquid-crystalline phase transition of the respective phospholipid under periodical vigorous vortex mixing. The peptides which were dissolved in the same buffer system were added together with the buffer during the preparation. The same hydration protocols were applied for liposomes with and without peptide.

Circular Dichroism

Measurements were performed at room temperature on a Jasco J 715 Spectropolarimeter (Jasco, Gross-Umstadt, Germany). Far UV-CD spectra were recorded at lipid-to-peptide molar ratio of

25:1 using quartz cuvettes with an optical path length of 0.02 cm. The CD was measured between 260 nm and 180 nm with a 0.2 nm step resolution. Each spectrum is the average of three scans to improve the accuracy. 4 mg/ml stock solutions of peptides were dissolved in 10 mM Hepes buffer and spectra measured in the presence of 20 mM sodium dodecyl sulfate (SDS) and 20 mM dodecylphosphocholine (DPC) to mimic some characteristics of cancer and healthy mammalian membranes. Respective backgrounds for each measurement were subtracted during the measurement. Percentage secondary structure calculations were done using Dichroweb, CDSSR Convolution Program using reference set 4 (Whitmore and Wallace, 2004; Whitmore and Wallace, 2008).

Differential Scanning Calorimetry

Differential scanning calorimetry (DSC) studies were performed with 2-dipalmitoyl-*sn*-glycero-3-phospho-L-serine (DPPS) and 1,2-dipalmitoyl-*sn*-glycero-3-phosphocholine (DPPC) lipids with the Microcal VP-DSC high-sensitivity differential scanning calorimeter (Microcal, Northampton, MA, USA). Individual experiments were repeated three times for the sample to reach thermodynamic equilibrium and second heating scan is taken into account for the data representation. Scans cover a range of 15 degrees above and 20 degrees below main transition temperature. All heating and cooling scans were recorded at a constant rate of 30°C/h. Pre-scan thermostating was set to 10 minutes for the heating scans and for 1 minute for the cooling scans. The total lipid concentration used for the DSC scans was 1 mg/ml. Data acquisition and analysis was done using Microcal Origin software (Microcal). Calorimetric enthalpies were calculated by integrating the peak areas after baseline adjustment and normalization to the mass of phospholipid. The phase transition temperature was defined as the temperature at the peak maximum where chain melting takes place.

Leakage of ANTS/DPX

Leakage of aqueous contents from liposomes was determined using the ANTS/DPX assay (Ellens et al., 1985b). As a first approximation to the charge density and exposed lipid head group property of a cancer cell membrane, negatively charged 1-palmitoyl-2-oleoyl-*sn*-glycero-3-phospho-L-serine (POPS) was used. As a healthy cell membrane mimic 1-palmitoyl-2-oleoyl-*sn*-glycero-3-phosphocholine (POPC) was used. Lipid films were hydrated with a buffer containing 12.5 mM ANTS, 45 mM DPX, 68 mM NaCl and 10 mM Hepes at pH 7.4 as describes above for DSC measurements. Differently, dispersions were extruded (Mini extruder, Avanti Polar Lipids Inc. Alabaster, Alabama USA) at least 21 times through a polycarbonate filter of 0.1 µm pore size at a temperature above their respective phase transition to obtain uniform large unilamellar vesicles (LUVs). Unencapsulated free ANTS/DPX was separated from the ANTS/DPX

containing vesicles by exclusion chromatography by the help of a separation column filled with Sephadex™ G-75. Afterwards, the phospholipid concentration was determined by phosphorus analysis so that peptide to lipid molar ratios in the measuring cuvette can be calculated. Fluorescence spectroscopy measurements were performed on a SPEX FluoroMax-3 spectrofluorometer (HORIBA Jobin-Yvon, Longjumeau, France) combined with Datamax software. Fluorescence intensity was observed at 37°C under constant stirring. Excitation and emission monochromators were set to 360 nm and 530 nm, respectively. Measurements were performed in a buffer containing 10 mM Hepes, 140 mM NaCl and 1 mM EDTA at pH 7.4. LUVs were added to the cuvette to achieve a final lipid concentration of 50 μM. Fluorescence emission was recorded as a function of time before and after the addition of incremental amounts of peptide to give a final concentration of 8 μM. The maximum level of fluorescence, determined by the lysis of the liposomes with Triton X-100, was assigned as 100% leakage.

Hemolysis

The hemolytic activity of the peptides were determined using human erythrocytes (group 0 rhesus positive) which was used within two days after collecting. Firstly, heparinized blood was centrifuged for three minutes at 2000 rpm then the supernatant was discarded and the pellet was washed with pH 7.4 PBS. The derived erythrocyte pellet was subsequently diluted with MES buffer (20 mM morpholinoethanesulfonic acid, 140 mM NaCl, pH 5.5 until 20 μL of this suspension added to 980 μL of double distilled water had the optical density of 1.4 at the wavelength of 412 nm. This value corresponds to 5×10^8 cells/ml. Equally, the peptides were diluted in MES buffer to the desired concentrations before 20 μL of the erythrocyte suspension was added to the 80 μL of peptide solution. As a control 20 μL of erythrocyte suspension was mixed with 80 μL of double distilled water, expecting 100% lysis of the erythrocytes. The negative control was prepared by mixing 20 μL of erythrocyte suspension and 80 μL of MES buffer where the lysis is zero. After mixing all samples carefully, the suspensions were incubated for 30 minutes at 37°C. Directly after incubation the samples were stored on ice and 900 μL MES buffer was added. All suspensions were centrifuged for ten minutes at 2000 rpm to sediment all intact erythrocytes. Finally, the absorbance was measured with a spectrometer (Tecan, Crailsheim, Germany) at 412 nm wavelength.

Computational Methods

Monte Carlo simulation of the interaction of a peptide molecule with POPS, POPC, and POPS/POPC membrane was performed as reported previously (Kessel et al., 2003;Shental-Bechor et al., 2005;Shental-Bechor et al., 2007). The peptide was described using a reduced representation with each amino acid represented as two interaction sites, one corresponding to the

alpha-carbon and the other to the side chain. The initial conformation of the peptides were modeled using the Nest program (Petrey et al., 2003) based on the structure of NK-Lysin from Protein Data Bank (entry 1NKL, model 1). The membrane was approximated as a hydrophobic profile, corresponding to the hydrocarbon region of the membrane. In addition, the model membrane included also surface charges, corresponding to the polar head groups, which interacted electrostatically with the titratable residues of the peptide, depending on their protonation state, using the Gouy-Chapman potential.

Assays for Biological Activity

Activity of peptides was studied on LNCaP and 3T3-NIH cell lines by using fluorescence spectroscopy and fluorescence microscopy.

Culture and Harvesting of Human Cell Line

The lymph-node carcinoma of the prostate (LNCAP) was kindly provided by Beate Rinner ZMF, Graz. NIH-3T3 mouse fibroblast cells were obtained from DSMZ GmbH. LNCaP cell line was cultured in RPMI 1640 supplemented with 10 % FBS, 2.5g/l glucose, 10 mM Hepes and 1 mM sodium pyruvate. The NIH-3T3 fibroblast cells were cultured in DMEM supplemented with 10% FBS and 4.5g/L glucose. All cell lines were grown at 37°C in a humidified atmosphere containing 5% CO₂. All culture media and supplements were from PAA Laboratories GmbH. Hepes was purchased from Invitrogen GmbH and cell culture flasks and plates were purchased from Nunc GmbH. Cell numbers were counted via hemocytometry. Cells were harvested by accutase treatment and centrifuged and re-suspended in medium or PBS depending on the experimental conditions.

PI-uptake assay

Freshly harvested LNCAP and NIH-3T3 cells were suspended in their respective medium to a density of 1×10^5 cells/100µL in a set of eppendorf tubes. Peptides and melittin were added in duplicates and cells were incubated for one hour at 37°C in a humidified atmosphere with 5% CO₂. At the end of the incubation time, 2 µL of propidium iodide (PI) was added to each Eppendorf tube and the suspension was further incubated for 5 minutes at room temperature in the dark. Fluorescence spectroscopy measurements were performed on a SPEX FluoroMax-3 spectrofluorometer (HORIBA Jobin-Yvon, Longjumeau, France) combined with Datamax software. Excitation and emission monochromators were set to 535 nm and 617 nm, respectively. Two concentrations of peptides were tested and each set of experiment was repeated at least 7 times. Baseline value (cell suspension with PI) was subtracted from each measurement and melittin at high concentration was used as a control for 100% PI uptake.

Time Dependent Cytotoxic Effect of NKCS Derived Peptides as shown by Fluorescence Microscopy

Freshly harvested LNCAP and NIH-3T3 cells were suspended in their respective medium and seeded to 8 well slides to a density of 1×10^4 cells/300 μ L/well. Cell cultures were grown to 75% confluence. One well of each cell type received sufficient peptide solution to yield a final concentration of 1×10^{-5} M peptide. One well for each experiment received 1×10^{-5} M melittin as a positive control. 2 μ L of PI was added and microscopy pictures were taken in every 5 minutes up to 1 hour. Cells containing PI are dead and emit red light, while live cells cannot take up PI and therefore no red dye can be observed. The same procedure was repeated in the presence of 3×10^{-5} M peptide.

In Vitro PS Exposure

Freshly harvested LNCAP and NIH-3T3 cells were suspended in their respective medium and seeded to 8 well slides to a density of 1×10^4 cells/300 μ L/well. Cultures of cell at 75% confluence were stained with the fluorescent dyes Annexin V and PI for detection of apoptotic and necrotic cells (Molecular Probes, Invitrogen).

Results and Discussion

Conformational Investigations: Circular Dichroism and Monte Carlo Simulation

To reveal the secondary structures of the peptides (see Table 1 for the sequences) two approaches were used. Experimentally we investigated the secondary structure formation by CD spectroscopy and theoretically we conducted Monte Carlo simulations to estimate the content of helicity.

NKCS	KILRGVSKKIMRTFLRRISKDILTGKK
NK-14	KILRGVSKKIMRTF
NK-14-2	KILRGVSKKIMRTFKILRGVSKKIMRTF
NK-15	LRRISKDILTGKK
NK-15-2	LRRISKDILTGKKLRRISKDILTGKK

Table 1 Amino acid sequences of the peptides. Negatively charged residues are shown in red, positively charged residues are shown in blue.

CD measurements were carried out in the presence of 20 mM SDS (cancer mimic) and 20 mM DPC (healthy cell mimic) in 10 mM Hepes buffer. Both surfactant concentrations are above their respective critical micellar concentrations. Micelles formed by SDS are used as a simple mimetic of negatively charged bilayers. As reviewed in Blondelle et al. (Blondelle et al., 1999) above its CMC, SDS has been reported to be a stabilizer of alpha helical conformations and therefore one should consider each peptide's helical tendency with respect to each other.

Initially the spectra of the peptides in water were recorded. Regarding all the peptides, a pronounced dip at around 198 nm and a positive peak at around 215 nm were observed which are indicative of a predominant random coil structure (data not shown).

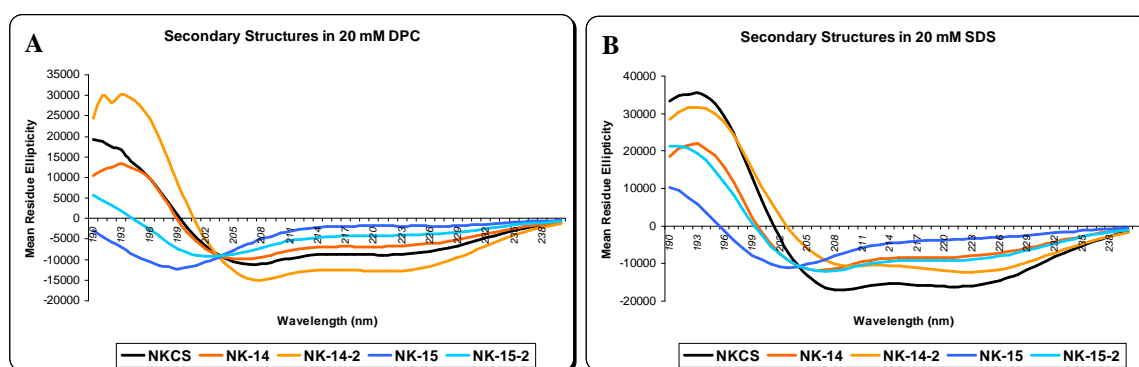


Figure 1 Circular dichroism spectra of NKCS and derived peptides in the presence of 20 mM SDS (A) and DPC micelles (B). Spectra recorded at a surfactant-to-peptide molar ratio of 25:1.

Upon addition of SDS in 10 mM Hepes, NKCS exhibited a characteristic double minimum at about 208 nm and 222 nm and a maximum around 194 nm, which indicate the presence of helical conformation. NK-14 spectrum showed the same property which is slightly shifted to lower wave length. NK-14-2 gave the same hallmarks of alpha helical signal showing maxima at 193 nm and a double minimum at 207 nm and at 223 nm which was significantly more pronounced than for its monomeric form NK-14 as well as NKCS. However, according to Dichroweb convolution (Whitmore and Wallace, 2004) latter appears as the most helical peptide. NK-15, the C-terminal segment, exhibited one minimum at 199 nm and convolution showed that it has the least helical content. The duplicate, NK-15-2, gave a spectrum which was marked by one minimum at 199 nm. According to the convolution program however duplication seems to increase the helical content more than two-fold as compared to its monomeric counterpart, NK-15. Considering all peptides, NK-15 has the highest propensity for beta structure in the presence of SDS micelles.

The same set of experiments was repeated in the presence of DPC micelles. The spectrum of NKCS and NK-14 showed two negative peaks at around 226 nm and 222 nm and one positive peak at around 193 nm which again indicates the presence of α -helical content. According to

Dichroic convolution, NKCS has a much lower helical content in DPC than SDS (31% and 59%, respectively); NK-14 however has a similar amount of helical content in these two environments. Duplication of the N-terminal peptide resulted in the highest helical content measured for any condition which is clearly shown from the spectra marked by double minimum at 206 nm and 223 nm and one maximum at 193 nm. As for the C-terminal segment, in the presence of DPC micelles, the helical content is negligible and random and beta structures are more prominent as shown by one negative peak at 199 nm. Duplication of N-terminal does not give rise to a significant amount of helical content.

	peptides	% alpha		% beta		% turn		% random	
		SDS	DPC	SDS	DPC	SDS	DPC	SDS	DPC
Parent peptide	NKCS	59	31	9	19	13	20	20	29
N-terminal segment	NK-14	35	30	20	22	20	20	25	27
Duplicate of N-terminal segment	NK-14-2	49	55	10	14	13	12	27	20
C-terminal segment	NK-15	13	6	30	33	25	26	34	35
Duplicate of C-terminal segment	NK-15-2	34	14	18	26	19	27	29	33

Table 2 Secondary structures of NKCS and derived peptides in cancer cell membrane mimic (SDS) and healthy mammalian cell membrane mimic (DPC) environments at a surfactant-to-peptide molar ratio of 25:1.

We can conclude that both C-terminal peptides tend to form random coil structures in the presence of DPC micelles while the N-terminal peptides together with NKCS tend to fold into alpha helical structures. Interestingly, NK-14-2 exhibited a similar amount of helicity in both types of micelles (DPC 55% and SDS 49%, respectively). As shown in Figure 2, duplication resulted in promotion of helicity for both terminal segments.

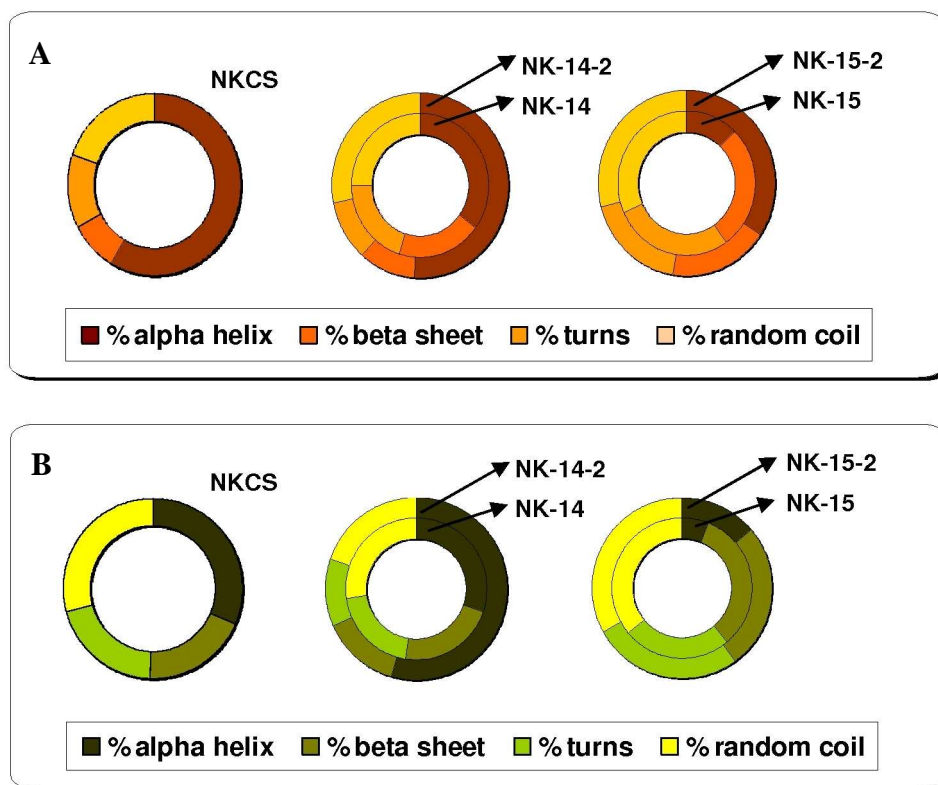


Figure 2 Percentage representation of α -helical, β -sheet, turn and random coil structures of NKCS and derived peptides in the presence of SDS micelles (A) and in the presence of DPC micelles (B) at a surfactant-to-peptide molar ratio of 25:1.

It should be kept in mind that both CD spectroscopy and the convolution program are designed for proteins but not for small stretches of peptides. Thus we assume they bear higher secondary structures than we observed and the values calculated for Figure 2 do not reflect the absolute α -helical content. However they can be used to compare the relative structuring of each peptide.

Computational Analysis: Monte Carlo (MC) Simulation

As shown in Figure 3 we calculated the predicted location of the peptides near bilayers for different lipid compositions (upper panel). The average distance of the α -carbon atoms from the bilayer mid-plane is shown for each residue. Keeping in mind that the polar heads' phosphate groups are located at the distance of 20 Å from the midplane of the bilayer, one can predict that none of the peptides interacts with the neutral lipid PC (black lines in Figure 3).

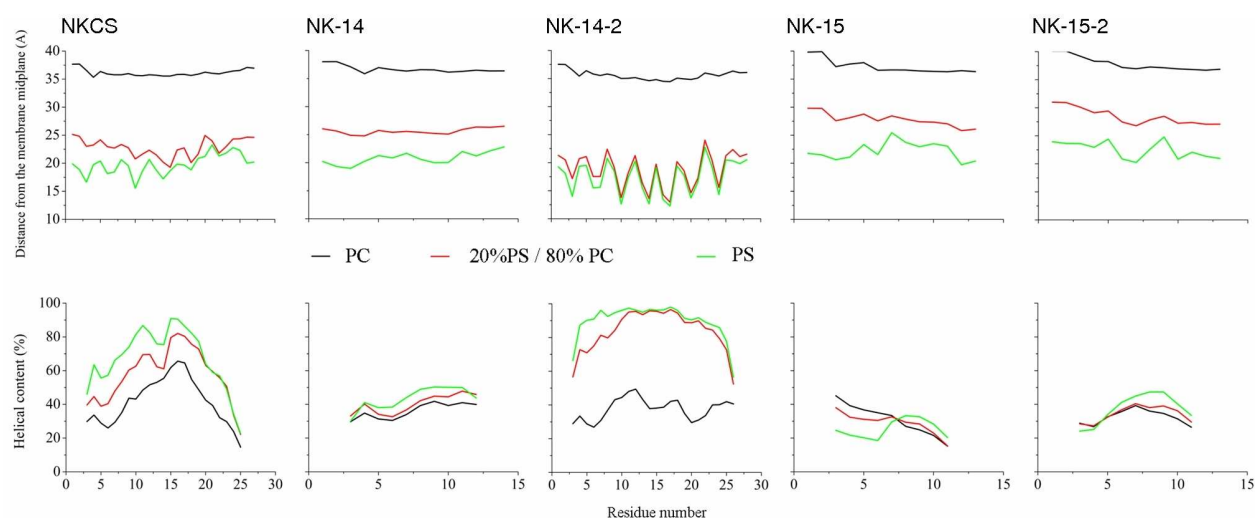


Figure 3 Upper panel shows the predicted location of the peptides near bilayers of different lipid compositions. Lower panel shows the computed helical content of the peptides near membranes of different compositions.

Both NKCS and NK-14-2 are, in average, inserted into the bilayers containing 20% and 100% negatively charged lipids. A closer look at the average conformations of the two peptides revealed that the hydrophobic residues (I, L, V) are located closer to the membrane mid-plane than polar and charged residues, suggesting their deeper penetration. This effect seems to be more pronounced for the dimeric peptide. Such conformation is favorable since it enables the hydrophobic residues to be buried in the hydrocarbon region of the bilayer, while the positively charged residues interact with the negative surface charge through Coulomb attraction.

In contrast, NK-15 and NK-15-2 rather remain in the aqueous phase even in the presence of a bilayer containing only the negatively charged lipid PS. Their predicted conformations show that the negatively charged surface faces with the positively charged residues. NK-14 is adsorbed on the surface of the bilayer made up of pure PS with the average conformation resembling NKCS and NK-14-2, and remains in water in the presence of the less negatively charged bilayer (20% PS) with the average conformation resembling NK-15 and NK-15-2.

Figure 3 lower panel shows the calculated helical content of the peptides near membranes of different compositions. The dihedral angles of two first and two last amino acids cannot be calculated, and are therefore omitted. The lower helical content peptides (NK-14, NK-15 and NK-15-2) near bilayers of three different compositions are in agreement with the upper panel showing no interaction between the peptides and the membranes.

The higher helical content of NKCS and NK-14-2 correlates with their penetration into the bilayer, being most prominent when they contain PS. It is important to note that the difference in helical content between neutral and charged lipid environments is the highest for NK-14-2.

Indeed, measured (CD) and calculated (MC simulation) helical structure propensities of the peptides correlate very well.

Binding Energies Calculated by Monte Carlo Simulation

We conducted preliminary MC simulations of NKCS and derivatives in the aqueous phase and in the presence of membranes composed of pure DPPC, pure DPPS and the cancer cell membrane mimic DPPS/DPPC mixture at a molar ratio of 2:8.

	NKCS	NK-14	NK-14-2	NK-15	NK-15-2
DPPC	1,71	0,22	1,35	0,60	0,17
DPPC/DPPS	-16,36	-5,56	-33,44	-2,16	-12,13
DPPS	-43,29	-20,32	-60,03	-14,35	-38,39

Table 3 The calculated membrane association free energies (kT) of the peptides.

Table 3 shows the calculated membrane association free energies. Low values of total free energy indicate strong interactions with the membrane, whereas relatively high free energy excludes membrane interaction suggesting that these peptides will not exhibit an anticancer activity. According to Table 3, NK-14-2 has the highest affinity towards DPPS containing membranes. The least active peptide for the cancer membrane mimic is NK-15. On the other hand, for the DPPC membrane, binding values vary in a very low range suggesting that difference in affinity cannot be large within these peptides.

To summarize the simulation study, one can conclude that helical structure propensity of the peptide is one of the determinants for its target membrane (DPPS including membrane) affinity. Free energy calculations also showed the benefit gained by the duplication of the N-terminal segment of the parent peptide. On the other hand, NK-14-2 associated with the DPPC membrane with a normal ranged free energy compared to the parent peptide, which means duplication did not result in a loss in membrane selectivity.

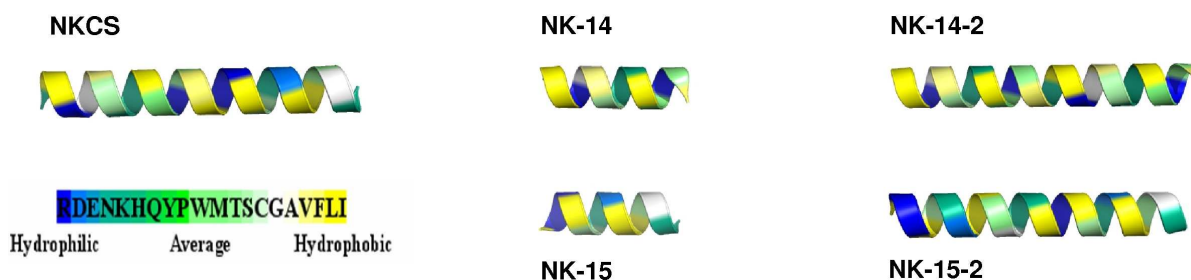


Figure 4 Compatibility of the NKCS and derivatives with an amphipathic canonical helical structure.

The ribbon structures of the peptides are represented according to the colored scale of hydrophobicity. The view is hydrophobic side facing the reader. NKCS has a compatible amino acid sequence with an amphipathic structure in which most of the hydrophobic residues align on one side of the helix. However it is indeed clear that NK-14-2 has a better compatibility with a canonical helical structure and almost all the hydrophobic residues align on one side of the helix drives a better insertion of the peptide into the bilayer. In the case of NK-15-2 the hydrophobic and hydrophilic residues are scattered in all directions around the helix and therefore it is not compatible with a canonical helical structure.

Membrane Permeabilization

The ability of peptides to permeabilize LUVs of different surface charge was tested by a dye release assay by using fluorescence spectroscopy. Peptide induced leakage, measured by a fluorescence quenching assay, is a well established technique for probing membrane activity of peptides (Almeida and Pokorny, 2009).

Peptide Mediated Leakage of ANTS/DPX from Liposomes

We used liposomes composed of zwitterionic POPC and of a mixture of negatively charged POPS and POPC (8:2 molar ratio of POPC/POPS) in order to mimic the outer layer of human erythrocytes membrane and cancer cell membrane respectively. Pure POPS liposomes used in order to unravel the affinity of peptides to PS alone. Full leakage is calculated according to the leakage caused by 50 mM Triton X-100.

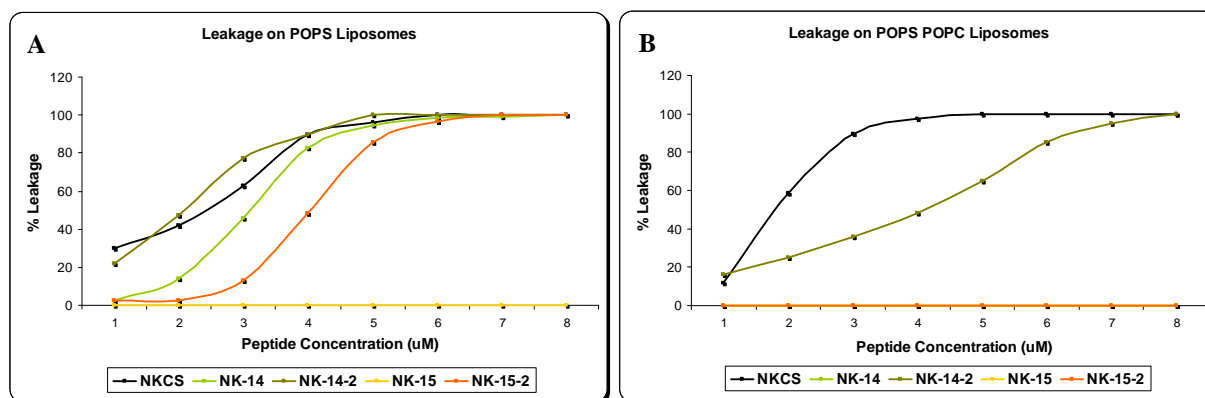


Figure 5 Leakage caused by cumulative addition of peptides to liposomes composed of POPS (A) and POPS/POPC (2:8 mol/mol) (B). Data show the effect of increasing peptide concentration starting from a lipid-to-peptide molar ratio of 50:1 (1 μ M) up to 6:1 (8 μ M).

At 37°C, addition of peptides starting from a lipid-to-peptide molar ratio of 100:1 (1 μ M) to POPS and POPS/POPC liposomes resulted in an increase of fluorescence emission in general

(Figure 5). Especially, addition of NKCS and NK-14-2 provoked a very abrupt increase, for that reason first phase could not be recorded. Addition of NKCS caused 100% leakage at 6 μ M on POPS liposomes, while NK-14-2 induced complete release at 5 μ M. Both NK-14 and NK-15-2 provoked full leakage at around 7 μ M, NK-15 did not stimulate any leakage at all concentrations. NKCS and NK-14-2 provoked full leakage on POPC/POPS liposomes however in a strikingly different manner than on POPS. Interestingly, NKCS invoked 100% leakage already at 4 μ M concentration while NK-14-2 reached full level of leakage only at 8 μ M. The other peptides were not active on the binary lipid system.

All the peptides were also tested on pure POPC liposomes (data not shown) only NK-14-2 invoked approximately 40% leakage at around 4 μ M and increasing concentration of the peptide did not result in any increase in the magnitude of the leakage.

Considering the secondary structures of the peptides, the most helical one, NK-14-2, appeared to be the most potent peptide on POPS liposomes. Seeing the fact that NK14-2 bears the highest helical content in the presence of DPC (55%), its effect on POPC liposomes emphasizes the importance of helicity.

Differential Scanning Calorimetry

As described before mammalian membranes are composed of different types of phospholipids. To simplify this complex system, single lipid model systems are initially chosen to investigate the effects of the peptides on the phospholipid phase transitions. Here we present the result of differential scanning calorimetry studies with DPPC and DPPS lipids. The heat capacity functions obtained for the pure lipid systems are consistent with previously published data (Sevcsik et al., 2008).

Effect of NKCS Peptides on Single-Component Lipid Systems

The heat capacity function of pure DPPS shown in Figure 6A is characterized by a highly cooperative main transition from the lamellar gel to the fluid phase ($L_{\beta} \rightarrow L_{\alpha}$) at 52,6°C and a minor transition which appears at 53,4°C.

The thermograms of DPPS liposomes recorded in the presence of NKCS peptides differ significantly from the one of pure DPPS. Most of the peptides induced overlapping transitions as can be deduced from the shape of the thermograms suggesting the presence of multiple membrane domains of varying peptide content. The respective thermodynamic parameters can be found in Table 4.

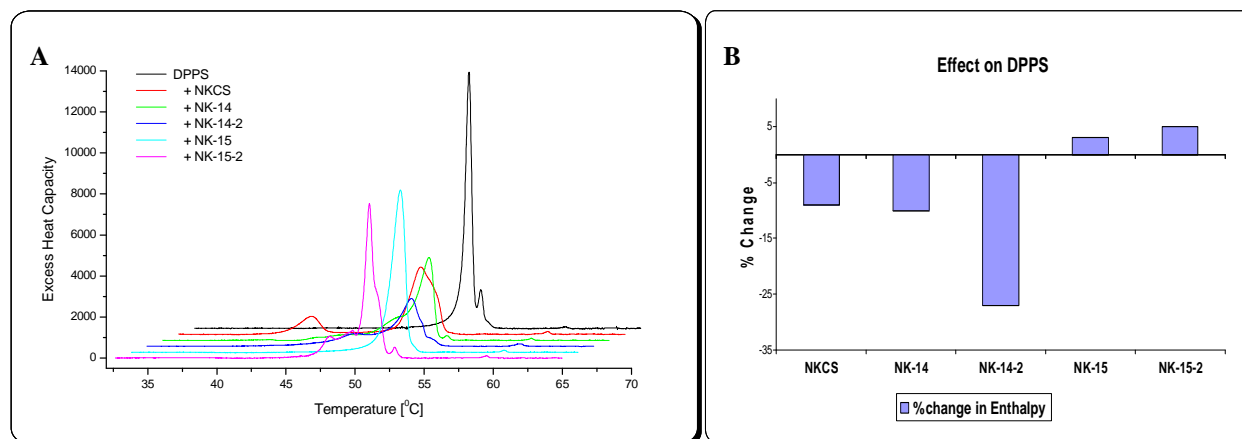


Figure 6 DSC thermograms of DPPS in the absence and presence of NKCS and derivatives at a lipid-to-peptide molar ratio of 25:1 (A). Change in total enthalpy in the presence of NKCS and derivatives (B).

All peptides tested lead to a decrease in the transition temperature indicating a perturbation of the lipid chain packing, whereby NKCS shifted the main transition temperature to lower values most strongly.

The N-terminal peptides together with NKCS caused a prominent decrease of the transition enthalpy, while the C-terminal peptides lead to a minor increase (see Figure 6B) which can be indicative for peptide-head group interaction.

	DPPS				
	T_1 (°C)	T_2 (°C)	T_m (°C)	ΔH_m (kcal/mol)	$\Delta T_{m1/2}$ (°C)
pure	n.a.	n.a.	52,6	10,0	0,53
+NKCS	42,3	n.a.	50,2	9,1	2,19
+NK-14	46,1	49,9	51,9	9,0	1,34
+NK-14-2	47,8	n.a.	51,8	7,3	1,88
+NK-15	n.a.	n.a.	52,2	10,3	1,09
+NK-15-2	48,2	49,8	51,0	10,5	0,7

Table 4 Thermodynamic parameters of DPPS in the absence and presence of NKCS and derivatives at a lipid-to-peptide molar ratio of 25:1. T_1 and T_2 (°C), transition temperature of peptide-enriched domains, T_m (°C), main transition temperature and its respective enthalpy (ΔH_m), and transition half-width ($\Delta T_{m1/2}$).

The heat capacity function of pure DPPC shown in Figure 7A is characterized by two phase transitions. The symmetric peak at 41,7°C corresponds to the main phase transition ($P_{\beta'} \rightarrow L_{\alpha}$) and the small peak appears at 35°C corresponds to the pre-transition ($L_{\beta'} \rightarrow P_{\beta'}$). Thermodynamic values are shown in Table 5.

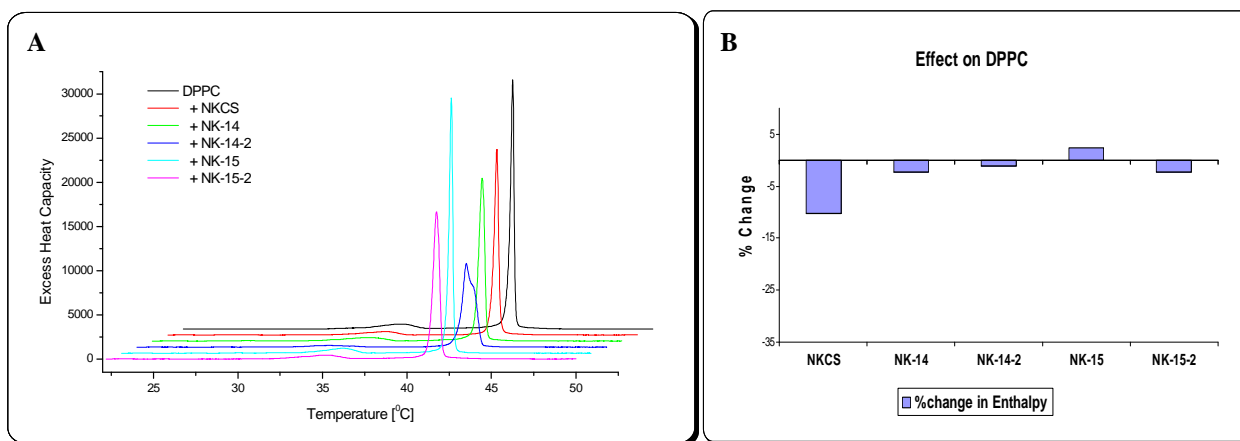


Figure 7 DSC thermograms of DPPC in the absence and presence of NKCS peptides at a lipid-to-peptide molar ratio of 25:1 (A). Change in main transition enthalpy in the presence of NKCS and derivatives (B).

The thermodynamic phase behavior of DPPC vesicles was not altered drastically in the presence of NKCS peptides which excludes a high degree of interaction. The presence of NKCS did not affect the pre-transition, however the main transition enthalpy decreased by 10%. Besides of NK-15, all peptides decreased the main transition enthalpy to different degrees. With the exception of NK-14-2, the peptides did not show any affect on pre-transition temperature.

Upon addition of NK-14-2 a broad peak appeared with the same maximum of the main transition temperature of the pure lipid and pre-transition temperature decreased 1,4°C. The latter observation can be explained by a loss of tilt of the hydrocarbon chains due to the interaction with the peptide which also decreased the pre-transition enthalpy by 60%. The pre-transition is usually more sensitive than the main transition to the presence of foreign molecules. Therefore we can conclude that amongst the peptides, NK-14-2 interacts with DPPC membrane more, which is in good agreement with the leakage data. Nevertheless the pre-transition did not abolish entirely. The slight increase in the enthalpy in the presence of NK-15 can be attributed to a lipid head group interaction of the peptide causing the head groups to pack tighter.

	DPPC					
	T_{pre} (°C)	ΔH_{pre} (kcal/mol)	$\Delta T_{pre/2}$ (°C)	T_m (°C)	ΔH_m (kcal/mol)	$\Delta T_{1/2}$ (°C)
pure	35,1	1,2	2,39	41,7	8,8	0,25
+NKCS	35,2	1,0	2,35	41,7	7,9	0,30
+NK-14	35,0	1,2	2,77	41,7	8,6	0,40
+NK-14-2	33,7	0,5	2,86	41,7	8,7	0,88
+NK-15	35,3	1,2	2,03	41,7	9,0	0,24
+NK-15-2	35,3	1,2	2,72	41,8	8,6	0,44

Table 5 Thermodynamic parameters of DPPC in the absence and presence of NKCS and derivatives at a lipid-to-peptide molar ratio of 25:1. Pre- and main transition temperature (T_{pre} , T_m), pre and main transition enthalpy (ΔH_{pre} , ΔH_m) and respective transition half width ($\Delta T_{pre/2}$, $\Delta T_{1/2}$).

Effect of NKCS peptides on Multi-Component Lipid System

In order to shed light on the preference of the peptides towards negatively charged lipids (PS) and neutral lipids (PC) we used a DPPC/DPPS mixture with a molar ratio of 8:2. The heat capacity function of this mixture is characterized by a single, highly cooperative transition at 43,1°C (Figure 8A).

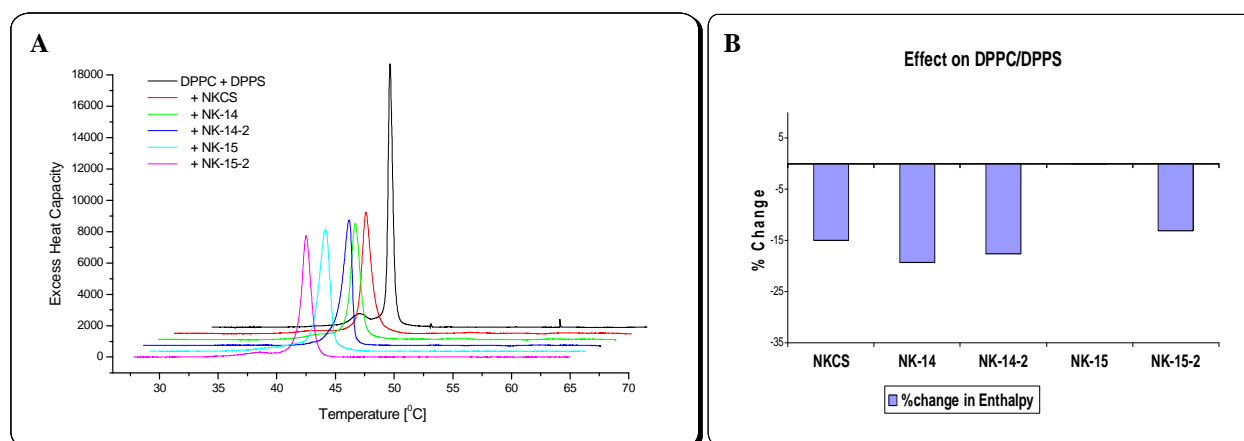


Figure 8 DSC thermograms of DPPC/DPPS (8:2 mol/mol) in the absence and presence of NKCS and derivatives at a lipid-to-peptide molar ratio of 25:1 (A). Change in main transition enthalpy in the presence of NKCS and derivatives (B).

Addition of peptides, with the exception of NK-15, resulted in a significant decrease in transition enthalpy (approx. 15%) accompanied by a decrease of transition cooperativity. NK-15

did not affect the enthalpy. No heterogeneous systems with a broad distribution of different domains were observed.

NK-14-2 had a dual effect on the heat capacity values. While it caused the strongest decrease in the enthalpy, 18%, the transition temperature increased slightly due to the stabilization of the gel phase. Presumably, the cationic peptide interacts preferentially with the negatively charged PS, therefore it leads to the depletion of PS from the PS/PC mixture causing main transition temperature to decrease and forming peptide-poor and peptide-rich domains. However here, on the contrary, we observed a slight increase in the main transition temperature and did not observe any domain formation. On the other hand, rest of the peptides decreased the main transition temperature only slightly.

	DPPC/DPPS		
	T_m (°C)	ΔH_m (kcal/mol)	$\Delta T_{1/2}$ (°C)
DPPS/DPPC	43,1	11,4	0,43
+NKCS	42,4	9,7	0,90
+NK-14	42,8	9,2	0,9
+NK-14-2	43,5	9,4	0,9
+NK-15	42,8	11,4	1,05
+NK-15-2	42,5	9,9	0,9

Table 6 Thermodynamic parameters of the binary lipid mixture DPPC/DPPS (2:8 mol/mol) in the absence and presence of NKCS and derivatives at a lipid-to-peptide molar ratio of 25:1. Main transition temperature (T_m), main transition enthalpy, (ΔH_m), and main transition half width ($\Delta T_{1/2}$).

In Vitro PS Exposure

Determination of PS surface exposure was carried out by annexin V binding assay. The human anticoagulant, annexin V is a 35-36 kD Ca^{2+} -dependent phospholipid binding protein which has a high affinity for PS. Annexin V is conjugated to Alexa Flour® 488 dye which emits green light (519nm) upon excitation. Dead cells were assessed by PI staining. PI is a polar compound that enters only the dead or dying cells when the plasma membrane is damaged. Once PI enters the cells, it forms complexes with DNA and induces intense red fluorescence (617 nm). As a result, live PS exposing cells show green fluorescence, live non-PS exposing cells show no fluorescence and dead cells show green and red fluorescence.

PS Exposure of LNCAP (lymph-node carcinoma of the prostate) Cell Line

As shown in Figure 9, the scattered green fluorescence dye observed under fluorescence microscopy indicates the accessible surface exposed PS on LNCaP cells. On the contrary, 3T3-NIH cells (murine originated fibroblast cells) exhibited PS only in the presence of disrupted cell membrane which is depicted by PI co-localization (Figure 10).

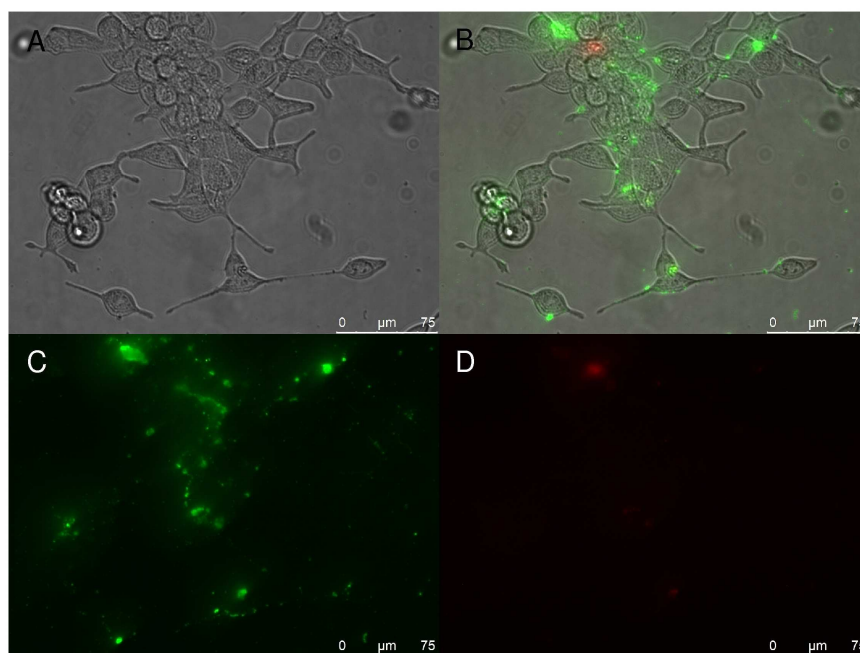


Figure 9 Fluorescence microscopy images of LNCaP cells simultaneously treated with Annexin V-Alexa Fluor 488 and PI. A; the bright field microscopy image of LNCaP cells, B; the combination image of three channels A, C and D. Annexin only staining is depicted in C and PI only staining is shown in D.

The difference between healthy and cancer cell membrane with respect to surface exposed PS is confirmed by microscopy. However, for a better quantification, the amount of bound annexin V must be assessed spectrofluorometrically.

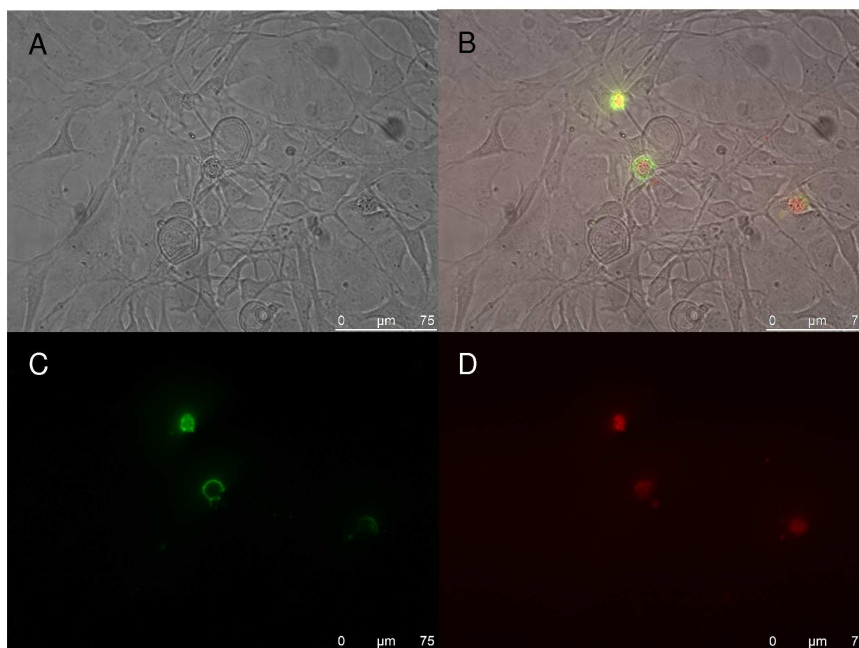


Figure 10 Fluorescence microscopy images of 3T3-NIH cells simultaneously treated with Annexin V-Alexa Fluor 488 and PI. A; the bright field microscopy image of 3T3-NIH cells, B; the combination image of three channels A, C and D. Annexin only staining is depicted in C and PI only staining is shown in D.

Biological Activity

Hemolytic activity was monitored by hemoglobin release from human erythrocytes and cytotoxicity of the peptides was assayed by PI-uptake against LNCaP and 3T3-NIH cell lines.

Hemolytic Activity and Cytotoxicity of Peptides

As shown in Figure 11, hemolytic activity was determined at three different concentrations (1 μM , 10 μM and 100 μM), Melittin served as a positive control. The data shown represent the average of three individual experiments performed in duplicates.

The peptides showed low hemolytic activity in comparison to melittin. At the highest concentration of 100 μM , NKCS and NK-14-2 caused lysis of 20% and 15% of red blood cells, respectively. It is well documented that the precursor peptide NK-2 exhibits low cytotoxicity against normal human lymphocytes (Schroder-Borm et al., 2005) but some hemolytic activity against human red blood cells (Andra et al., 2007). It is obvious that both NKCS and the newly derived peptides have less toxic effect on erythrocytes than the precursor peptide NK-2.

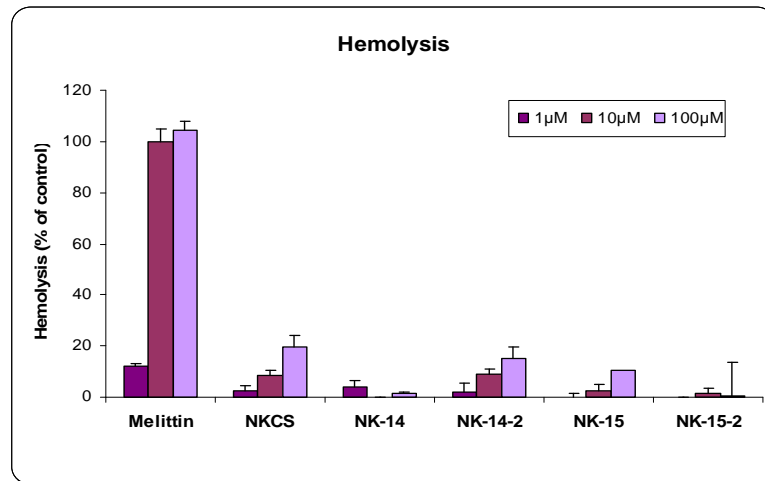


Figure 11 Hemolytic activity of NKCS and derivatives against human erythrocytes. Graph shows the effect of three different concentrations of peptide (1 μM , 10 μM and 100 μM) in comparison with melittin as a positive control. Concentration of cells: 5×10^8 cells/ml.

Cytotoxicity of the peptides was measured by using the uptake of the fluorescent exclusion dye PI. Two peptide concentrations, 10 μM and 30 μM , were tested with an incubation time of 1 hour against both cell lines, LNCaP and 3T3-NIH. The data shown represent the average of seven individual experiments performed in duplicates.

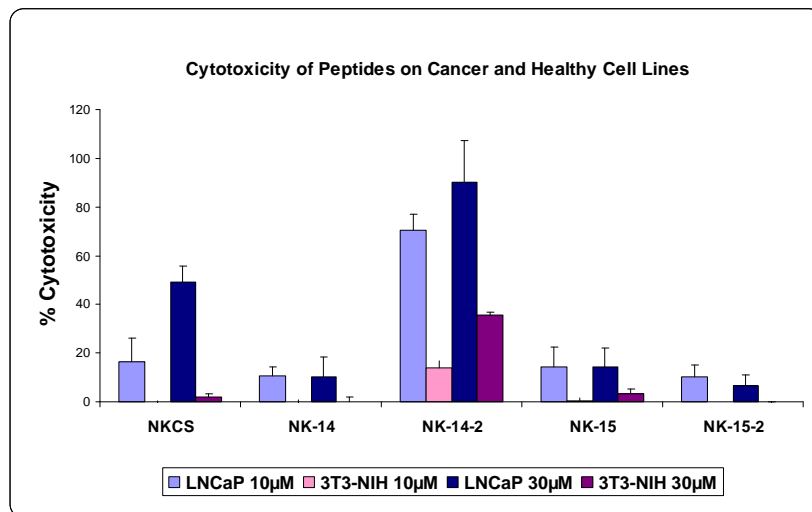


Figure 12 Cytotoxic activity of NKCS and derivatives determined by the PI-uptake assay. 10 μM and 30 μM peptides were tested against LNCaP (shown in light and dark blue, respectively) and 3T3-NIH cells (shown in light and dark pink, respectively).

The results show that the N-terminal duplicate, NK-14-2, exerted significant toxicity against cancer cells as compared to other peptides including the parent peptide. The PI-uptake in the presence of NK-14-2 was the highest at both concentrations (70% and 90% respectively). The anti tumor activity of the parent peptide was not retained in the rest of the newly derived peptides.

Except of NK-14-2 the peptide derivatives displayed slightly lower, almost similar anticancer activity compared to NKCS at 10 μM concentration. Unexpectedly, increasing the concentration of these peptides (NK-14, NK-15 and NK-15-2) did not result in increased toxicity. Toxicity against fibroblast cells was only observed for NK-14-2 which caused 14% cytotoxicity on 3T3-NIH cells at 10 μM concentration and 35% toxicity at 30 μM concentration.

In an attempt to understand the mass effect, duplicates of the N and C terminal segments were synthesised. At 10 μM peptide, duplication of N-terminal resulted in approximately 7-fold higher anticancer activity than the N-terminal alone and about 3-fold as compared to the parent peptide. Regarding the higher concentration, the benefit was less pronounced. Duplication of C-terminal however did not result in any significant increase of activity. Thus, we propose that increasing the peptide mass is not the dominant factor in respect of membrane and hence anticancer activity.

To sum up, duplication of N-terminal surely promotes higher activity towards cancer cells and evoked 5-fold selectivity. Nevertheless, the increasing toxicity exerted on NIH-3T3 cells should be evaluated separately. Microscopic examination displays no PS exposure on fibroblast cell line; which suggests that PI-uptake may be due to the experimental protocol resulting in some injured cells before peptide application. Moreover, the hemolytic assay shows no difference between the hemolytic activity of NKCS and NK-14-2. Further studies with miscellaneous cells lines and different toxicity assays are needed to conclude on more reliable selectivity measures. On the other hand, regarding an *in vivo* application there are multiple application approaches to target the desired site of action.

Kinetics of Cytotoxicity as Shown by Microscopy

The cells were tested for their viability and survived up to 2 hours without any visible damage under microscopy. In contrast, melittin caused a rapid killing starting immediately after the addition of the peptide. 100% toxicity was exerted in less than 30 minutes. (Figure 13-15: images were selected for 10 minutes intervals up to 50 minutes for simplicity).

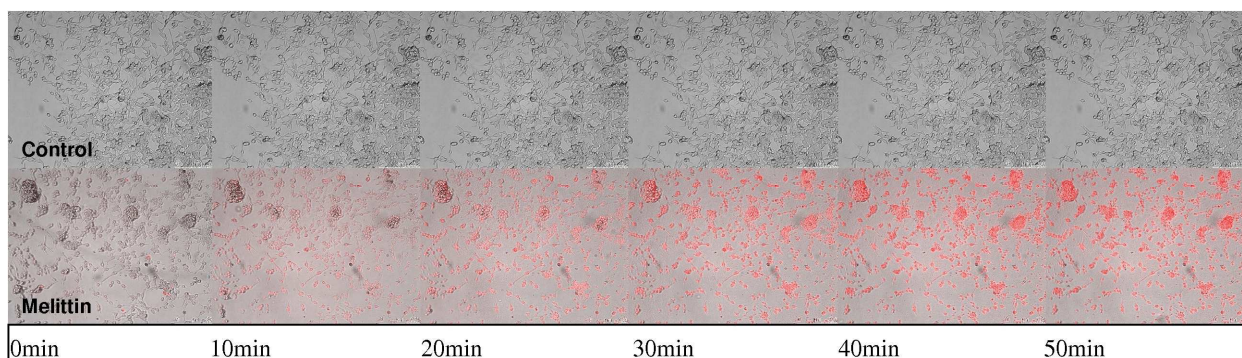


Figure 13 Real-time fluorescence microscopy images of LNCaP cells incubated with 30 μM melittin in the presence of PI.

In Figure 14, cells were exposed to 30 μM peptide and imaged continuously for 1 hour under the fluorescence microscope in the presence of PI. NK-14-2 showed the same trend like melittin and dead cells were already observed within 10 minutes, while the parent peptide NKCS developed toxicity only around 20 minutes. However, unlike melittin and NK-14-2, in the presence of NKCS no 100% toxicity was achieved within the observation period of 50 minutes. In each case the toxicity arose in less than an hour, which is fairly short and seems to exclude any receptor mediated killing mechanism.

The microscopy pictures from this assay appear to indicate that the damage caused by the peptides is more severe than that indicated by previous PI-uptake assay.

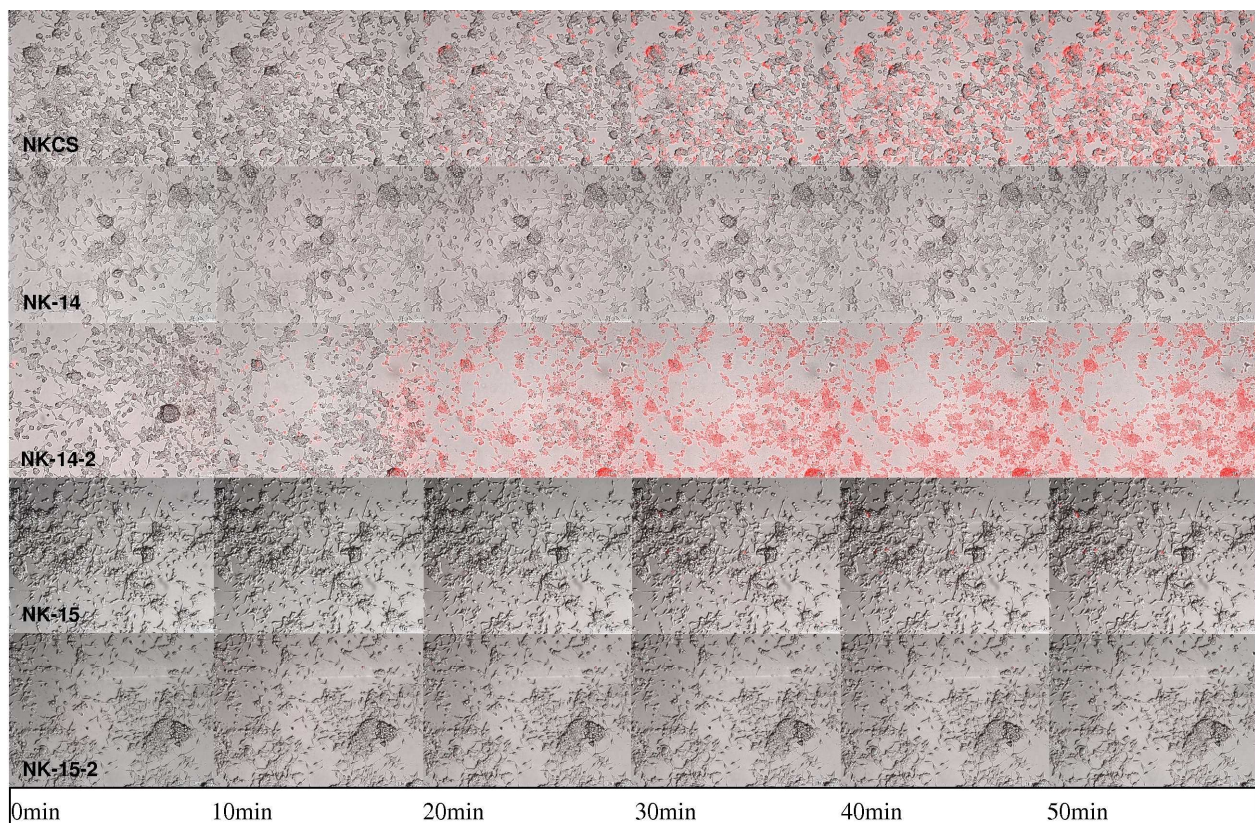


Figure 14 Real-time images of cytotoxicity of NKCS and derivatives. LNCaP cells incubated with 30 μM peptides in the presence of PI for 50 minutes.

Figure 15 shows the toxicity evoked on 3T3-NIH cells by the most active peptides in comparison to melittin. Melittin again causes 100% killing however in a delayed manner compared to LNCaP. NKCS and NK-14-2 showed insignificant killing which is also much less than observed by the PI-uptake assays.

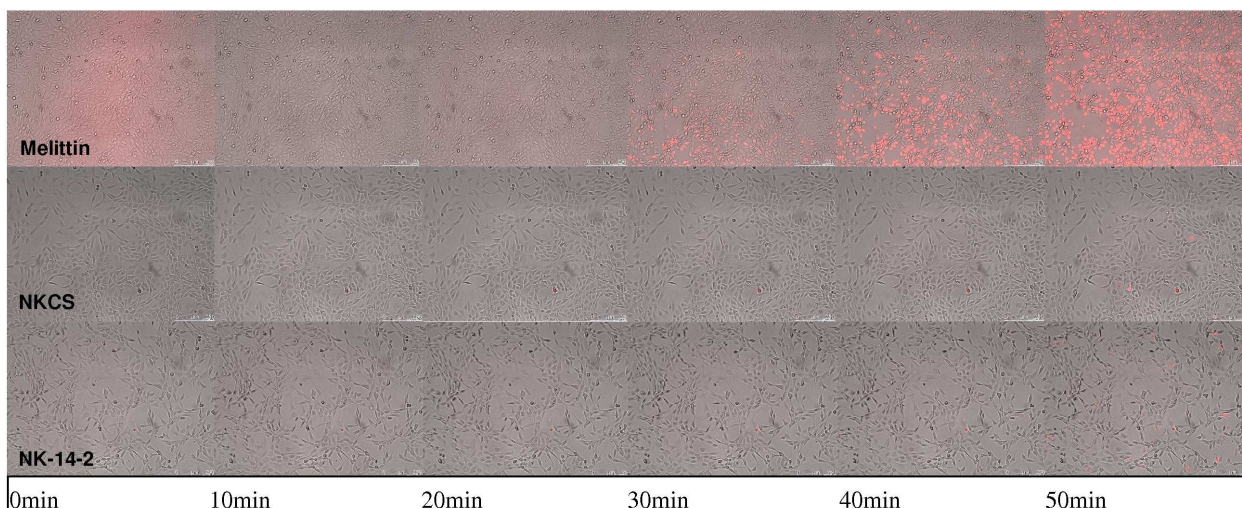


Figure 15 Real-time images of cytotoxicity of NKCS and NK142 in comparison to the cytotoxic melittin. 3T3-NIH cells incubated with 10 μ M peptides in the presence of PI for 50 minutes.

Conclusion

Current anticancer drugs such as, alkylating agents, metabolites and natural products, display little or no selectivity towards healthy mammalian cells and therefore they cause drastic side effects (Schweizer, 2009). There is an immediate need to develop a selective anticancer therapeutic regime that evokes reduced toxicity with a novel mode of action. Increasing amount of information referring to anti cancer peptides has not yet been translated into concepts concerning their mechanism of action. In order to shed light on the variables of a potent anti cancer peptide we conducted this study with NKCS and peptides derived thereof.

We have synthesized dimers of the N-terminal as well as C-terminal segment of NKCS and compared their properties with their monomers and the parent peptide. We investigated their secondary structure in various environments, their interaction with model membranes mimicking cancer and healthy cell membranes and tested their cytotoxic activities against cancer cells. Their cytotoxicity on fibroblast cells together with hemolysis assay unraveled their selectivity. To correlate the results of these different approaches with the physicochemical properties of the peptides we summarized their activity in Table 7. Despite an overall good agreement between the results gained by the various techniques applied, there are still some open questions which necessitate further investigations. However, in general, one can conclude that the C- and N-terminal segment were not as active as the parent peptide. While duplication of the N-terminal segment resulted in a higher activity as compared to NKCS, duplication of the C-terminal segment did not improve the weak activity of the monomeric form.

Peptide	Sequence	n	Q	μ	H (%)	α (%) SDS	α (%) DPC	Leakage (100%)	Cyto-toxicity (%)	Hemo-lysis (%)
NKCS	KILRGVSKKIMRTFLRRISKDILTGKK	27	+10	5,12	37	59	31	5 μ M	16,5	8,4
NK-14	KILRGVSKKIMRTF	14	+6	4,92	42	35	30	8 μ M	10,5	0
NK-14-2	KILRGVSKKIMRTFKILRGVSKKIMRTF	28	+11	9,25	42	49	55	6 μ M	70,4	9,2
NK-15	LRRISKDILTGKK	13	+5	3,18	30	13	6	n.a.	14,2	2,4
NK-15-2	LRRISKDILTGKKLRRISKDILTGKK	26	+9	2,19	30	34	14	8 μ M	10,4	1,3
Melittin	GIGAVLKVLTTGLPALISWIKRKRQQ	26	+6	5,18	46	n.a.	n.a.	n.a.	100	100

Table 7 Sequence and physicochemical parameters of NKCS and derived peptides (length (n), net positive charge (Q), hydrophobic moment (μ), total hydrophobic ratio (H)), α -helical content in SDS and in DPC micellar environment as well as leakage and biological activity (peptide concentration causing % 100 leakage of POPS vesicles, amount of cytotoxicity on LNCaP cells as measured by PI-uptake assay and hemolysis evoked by 10 μ M peptides).

Cationicity and length are important features of anti cancer peptides (ACPs). Based on a study of lactoferricin derived peptides, a sequence composed of 14 amino acids and a net positive charge of +7 was reported to be the optimum for high anticancer activity (Yang et al., 2004). Our amino acid sequence varies from these peptides and as a consequence we oppose that statement and point out that the specific residue composition of an ACP has to be considered, as they determine other important variables for membrane interaction such as hydrophobicity or hydrophobic moment. In our case, we observed the best activity for the 28 amino acid peptide, NK-14-2, with a net positive charge of +11. The hydrophobic moment of NK-14-2 is the largest amongst the peptides including melittin, but still selectivity was observed. A high hydrophobic moment thus does not hinder the selectivity which an ACP must exert. On the other hand, the hydrophobic ratio does not explain much about the activity or selectivity either, since it only depends on the number of hydrophobic residues with respect to the whole sequence. A small stretch of peptide can bear a high hydrophobic ratio while the peptide length may not be enough for activity.

In agreement with previous studies (Sebastian Linser, 2006;Gofman et al., 2010;Linser, 2006) helicity definitely affects the activity of an ACP. CD results showed that NKCS and derivatives were unstructured in water but adopted secondary structures in the presence of lipidic

micelles. Although NKCS exhibited the most helical structure in SDS environment, NK-14-2 showed higher activity in *in-vitro* tests as well as in leakage studies on POPS liposomes. This can be explained by the higher hydrophobic moment of the latter peptide. Results from Monte Carlo simulation are in agreement with these observations indicating the highest binding affinity as well as deepest insertion into PS containing bilayers for NK-14-2.

Interestingly, it was reported that Arg is more important than Lys in short peptides for antibacterial activity (Yang et al., 2004). Moreover, there is no Ala in NKCS and derived peptides which is known to be a helix stabilizer. However, regarding ACPs, there has been no such amino acid preference reported so far. Nevertheless, a well-defined secondary structure - α -helix - enables the separation of polar and non-polar amino acid residues along the helix creating an amphipathic structure. While it is in dispute for antibacterial activity, such a structure is indispensable for a potent ACP (Schweizer, 2009). The amphipathic nature of HDPs favors their intercalation into the bilayer which can result in perturbation of the membrane structure. We evaluated the potential amphipathicity of NKCS derived peptides by plotting them in canonical helical structures. Thereby, NK-14-2 showed the best compatibility with an ideal amphipathic helix (Figure 4). The width of the cationic and hydrophobic sectors, respectively, can be evaluated from the helical wheel projection as shown in Figure 16. As can be deduced from this projection, NK-14-2 exhibits an ideal separation of polar and non-polar residues and has a larger hydrophobic sector than its parent peptide. In accordance with its lack of anticancer activity, NK-15-2 shows no well defined amphipathic character.

Hemolysis assay and cytotoxicity as shown by microscopy proved a good degree of selectivity for NK-14-2 which can be attributed to its ability to target surface exposed PS on LNCaP cells. This is in line with biophysical data demonstrating its affinity to PS containing over zwitterionic lipids. The data obtained with NKCS and NK-14-2 support the view that diminished membrane interactions of selective ACPs with zwitterionic lipids accounts for their low hemolytic activity (Dathe et al., 2002). PI-uptake assay showed that cytotoxicity increases with increasing concentration of NKCS and NK-14-2. However, the selectivity gain is much better at lower peptide concentration. The C-terminal peptides showed no activity on cancer cells. Interestingly, NK-15 was shown to be inactive against bacteria as well (Linser, 2006).

Normal and tumor cells are different in their cytoskeleton and membrane organizations which lay the basis of differential effects of ACPs (Arlotti et al., 2001). It was deduced that the cytoskeletal alterations resulting from transformation of the cells render them susceptible to the cytolytic activity evoked by ACPs, primarily by causing a loss of osmotic stability. Thus a steady cytoskeletal system as possessed by normal cells could account for the resistance to the lytic effects of the peptides (Jaynes et al., 1989). The rapid and strong membranolytic effect of NK-14-2 should circumvent established resistance mechanisms. Furthermore, since the overall mechanism is dramatically different than that of conventional chemotherapeutic agents, they may

function synergistically. Therefore drug combination therapies with NK-14-2 should also be considered in further developments. Given the low concentration and unique mode of action of our newly designed peptide, it is possible to enhance the administration of the molecule with the help of nanotechnology directed therapies which would amplify its therapeutic value and limit toxicity to non cancerous cells.

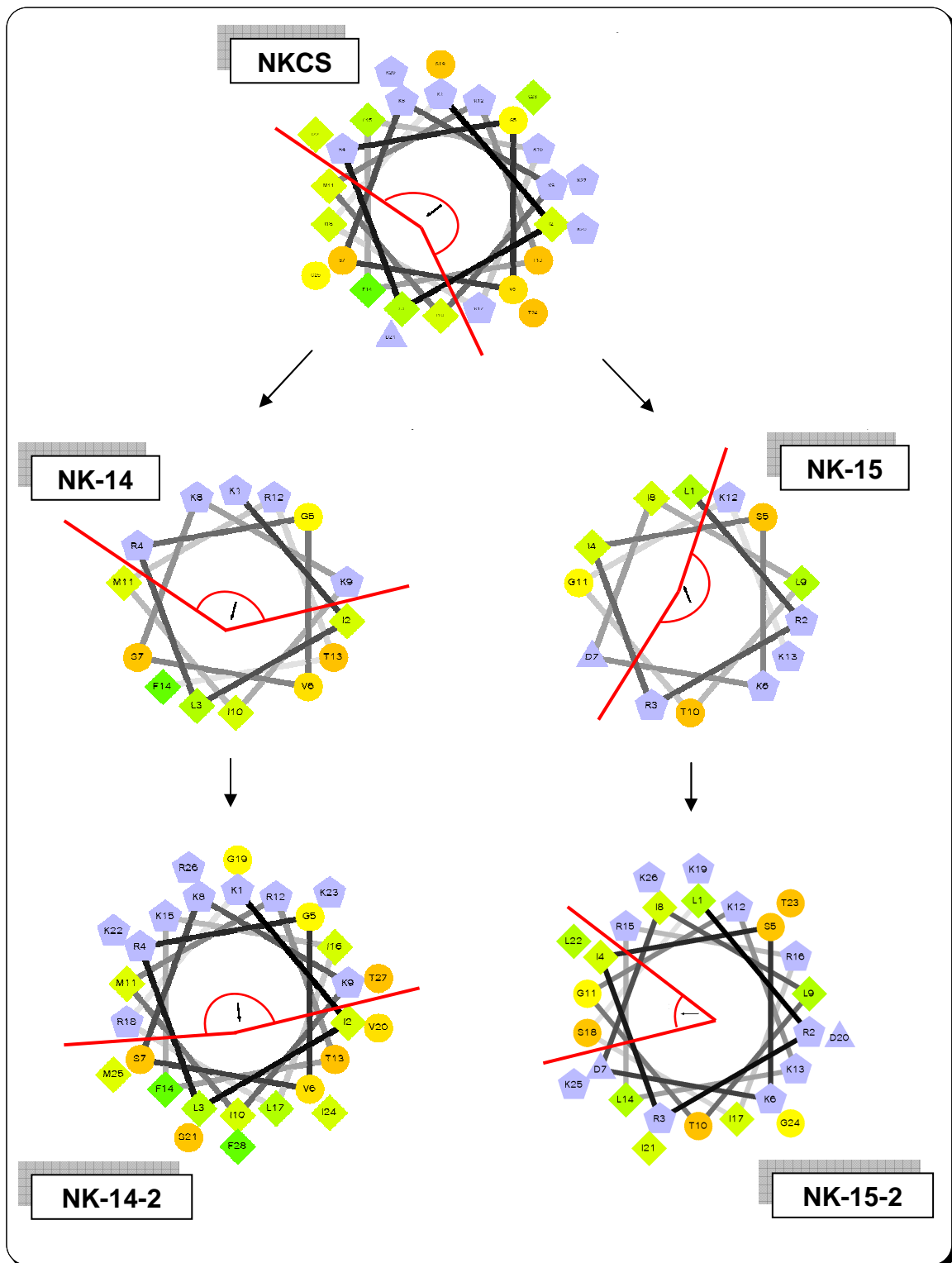


Figure 16

Schematic sketch of the development of NKCS derived peptides together with their helical wheel representations. Format code: Circles are hydrophilic, diamonds are hydrophobic, triangles are potentially negatively charged and pentagons are potentially positively charged residues. Color code: Zero hydrophobicity is yellow, the amount of hydrophobicity increases as the green color increases. Hydrophilic residues are red and the amount of red decreases as the hydrophilicity decreases. Potentially charged residues are light blue. Arrows indicate the angle of the hydrophobic moment (Zidovetzki et al., 2003) The cationic sector is marked by a red line.

Chapter 3

Summary and Outlook

Initially emerged as antimicrobial peptides, HDPs have a wide variety of existence in nature. They are mostly membrane active peptides and produced within the innate immune system by almost all species of living organisms (Hancock and Lehrer, 1998). Since their discovery and isolation, HDPs have been studied extensively in respect of their antimicrobial activity. Recently, it has been shown that some HDPs also have anticancer activity and may be used as promising anticancer agents (Schweizer, 2009). Neoplastic process results in many changes, one of which is the flipping of PS to the outer leaflet of the cell membrane. This anionic lipid serves as a target for HDPs. The electrostatic attraction between the anionic lipid molecule and cationic peptide is believed to play a role in the selective disruption of the plasma membrane. However, it is still not known, why some peptides are toxic to cancer cells while some are not (Hoskin and Ramamoorthy, 2008). Moreover, structural determinants that make an HDP cancer specific are mainly unknown.

We used various biophysical techniques, Monte Carlo simulation and *in vitro* assays to study the anticancer properties of NKCS, a derivative of the antimicrobial peptide NK-2. NKCS is known to be composed of two helices connected with a hinge region. We synthesized the individual helices and tested them on model lipid bilayers to evaluate the extent of specific interaction with PS and neutral PC. In the first part of this thesis we showed that the N-terminal segment of NKCS (NK-14) exhibits a helical structure in membrane mimetic environment, while the C-terminal segment (NK-15) had only a negligible amount of α -helix. Moreover, NK-14 is characterized by a higher amphipathicity and in contrast to NK-15 induced leakage of liposomes containing PS. NK-15 showed no prominent interaction with bilayers composed of PS or PC. Therefore, we concluded that the N-terminal segment is responsible for the PS affinity of the parent peptide and that an amphipathic helical structure favours anticancer activity.

In the second part of this thesis we extended the studies to the dimeric form of the N- and C-terminal peptide segments, termed NK-14-2 and NK-15-2 respectively, and compared their behaviour to their parent peptide NKCS. Monte Carlo simulation showed that only NKCS and NK-14-2 significantly insert into the lipid bilayer with an active helical conformation. These findings correlate well with observations from CD, calorimetric and leakage experiments showing that NK-14-2 was most effective in perturbing the bilayer structure and in inducing leakage of PS containing liposomes. NK-14-2 exhibits the most helical structure amongst the

peptides tested and fits properly to a canonical helix displaying full amphipathicity which was found to be indispensable for membrane insertion resulting in membrane damage and hence anticancer activity of NKCS derived peptides. Monte Carlo simulations suggested an orientation of the peptides parallel to the membrane plane which has to be proven experimentally. One technique to address this problem is ATR-FTIR spectroscopy on oriented lipid bilayers. Therefore, such studies using different lipid matrices and peptide concentrations reflecting the leakage experiments have been initiated.

The aforementioned membrane insertion of the peptide may also cause the collapse of electrochemical potential across the membrane which results in necrotic killing of the cell. Moreover, it has been known that malignancy formation is often associated with an increase of superficial membrane potential (Dobrzynska et al., 2005). Therefore, malignancy transformation can render cells more susceptible to ACP killing. From this respect, the effect of the newly derived peptides on plasma membrane potential of cancer cells should be further evaluated. After all, it has been suggested that dependent or independent of the malignancy phase of the cancer cell, peptide killing mechanism includes membrane depolarization (Papo et al., 2004; Arlotti et al., 2001). It should be mentioned that some cationic amphiphilic peptides can cross the cytoplasmic membrane and cause swelling of mitochondria which then induces the apoptotic pathway (Mai et al., 2001). To exclude such a mechanism for NKCS derived peptides further tests have to be performed to assess the induction of apoptotic pathway by the help of a DNA laddering assay or by one of the commercial kits which are available to follow apoptosis based on caspase function.

Regarding PS sidedness, we showed its exposure on the outer plasma membrane leaflet of prostate cancer line. However, in order to conclude on a direct correlation between the amount of PS exposed and the activity of the peptide, the amount of exposed PS must be assessed quantitatively by the help of Annexin V binding assay with the use of FACS analysis or spectrofluorometer. Furthermore, co-localization of PS and peptide should be studied with fluorescence spectroscopy experiments. Thereby, rhodamine labelled NK-14-2 and PS tagged by FITC-Annexin V would help to show the direct and selective interaction between the two molecule species. So far, we only focused on PS exposure. However, as mentioned above there are fundamental differences between cancer cells and normal cells. In order to shed light onto the mechanism of action and efficacy of ACPs their interaction with other anionic molecules located on the cancer cell surface such as O-glycosylated mucins, sialated ganglioside and heparan sulfates must be extensively studied.

Finally, *in vitro* assay based on PI-uptake showed the activity and selectivity of NK-14-2 both spectroscopically and microscopically. However, in order to obtain an IC_{50} value, a quantitative assay has to be conducted such as MTT assay to yield a pharmacologically more relevant parameter.



Chapter 4

Reference List

Almeida,P.F. and A.Pokorny. 2009. Mechanisms of antimicrobial, cytolytic, and cell-penetrating peptides: from kinetics to thermodynamics. *Biochemistry* 48:8083-8093.

Anderson,D.H., M.R.Sawaya, D.Cascio, W.Ernst, R.Modlin, A.Krensky, and D.Eisenberg. 2003. Granulysin crystal structure and a structure-derived lytic mechanism. *J. Mol. Biol.* 325:355-365.

Andersson,M., H.Gunne, B.Agerberth, A.Boman, T.Bergman, R.Sillard, H.Jornvall, V.Mutt, B.Olsson, H.Wigzell, and . 1995. NK-lysin, a novel effector peptide of cytotoxic T and NK cells. Structure and cDNA cloning of the porcine form, induction by interleukin 2, antibacterial and antitumour activity. *EMBO J.* 14:1615-1625.

Andra,J. and M.Leippe. 1999. Candidacidal activity of shortened synthetic analogs of amoebapores and NK-lysin. *Med. Microbiol. Immunol.* 188:117-124.

Andra,J., D.Monreal, d.T.Martinez, C.Olak, G.Brezesinski, S.S.Gomez, T.Goldmann, R.Bartels, K.Brandenburg, and I.Moriyon. 2007. Rationale for the design of shortened derivatives of the NK-lysin-derived antimicrobial peptide NK-2 with improved activity against Gram-negative pathogens. *J. Biol. Chem.* 282:14719-14728.

Arlotti,J.A., T.S.Cimino, T.Nguyen, R.Dhir, A.Thomas, J.M.Jaynes, A.L.Caldwell, and R.H.Getzenberg. 2001. Efficacy of a synthetic lytic peptide in the treatment of prostate cancer. *Urol. Oncol.* 6:97-102.

Bechinger, B. and K. Lohner. 2006. Detergent-like actions of linear amphipathic cationic antimicrobial peptides. *Biochim. Biophys. Acta* 1758:1529-1539.

Beleznay, Z., A. Zachowski, P.F. Devaux, M.P. Navazo, and P. Ott. 1993. ATP-dependent aminophospholipid translocation in erythrocyte vesicles: stoichiometry of transport. *Biochemistry* 32:3146-3152.

Bello, J., H.R. Bello, and E. Granados. 1982. Conformation and aggregation of melittin: dependence on pH and concentration. *Biochemistry* 21:461-465.

Bevers, E.M., P. Comfurius, and R.F. Zwaal. 1983. Changes in membrane phospholipid distribution during platelet activation. *Biochim. Biophys. Acta* 736:57-66.

Bevers, E.M., P. Comfurius, and R.F. Zwaal. 1996. Regulatory mechanisms in maintenance and modulation of transmembrane lipid asymmetry: pathophysiological implications. *Lupus* 5:480-487.

Bevers, E.M. and P.L. Williamson. 2010. Phospholipid scramblase: An update. *FEBS Lett.*

Bitbol, M., P. Fellmann, A. Zachowski, and P.F. Devaux. 1987. Ion regulation of phosphatidylserine and phosphatidylethanolamine outside-inside translocation in human erythrocytes. *Biochim. Biophys. Acta* 904:268-282.

Blattman, J.N. and P.D. Greenberg. 2004. Cancer immunotherapy: a treatment for the masses. *Science* 305:200-205.

Blondelle, S.E., K. Lohner, and M. Aguilar. 1999. Lipid-induced conformation and lipid-binding properties of cytolytic and antimicrobial peptides: determination and biological specificity. *Biochim. Biophys. Acta* 1462:89-108.

- Bruckheimer,E.M. and A.J.Schroit. 1996. Membrane phospholipid asymmetry: host response to the externalization of phosphatidylserine. *J. Leukoc. Biol.* 59:784-788.
- Burdick,M.D., A.Harris, C.J.Reid, T.Iwamura, and M.A.Hollingsworth. 1997. Oligosaccharides expressed on MUC1 produced by pancreatic and colon tumor cell lines. *J. Biol. Chem.* 272:24198-24202.
- Cassidy,J. and J.L.Misset. 2002. Oxaliplatin-related side effects: characteristics and management. *Semin. Oncol.* 29:11-20.
- Chaudhary,J. and M.Munshi. 1995. Scanning electron microscopic analysis of breast aspirates. *Cytopathology* 6:162-167.
- Chavakis,T., D.B.Cines, J.S.Rhee, O.D.Liang, U.Schubert, H.P.Hammes, A.A.Higazi, P.P.Nawroth, K.T.Preissner, and K.Bdeir. 2004. Regulation of neovascularization by human neutrophil peptides (alpha-defensins): a link between inflammation and angiogenesis. *FASEB J.* 18:1306-1308.
- Chen,H.M., W.Wang, D.Smith, and S.C.Chan. 1997. Effects of the anti-bacterial peptide cecropin B and its analogs, cecropins B-1 and B-2, on liposomes, bacteria, and cancer cells. *Biochim. Biophys. Acta* 1336:171-179.
- Chen,J., X.M.Xu, C.B.Underhill, S.Yang, L.Wang, Y.Chen, S.Hong, K.Creswell, and L.Zhang. 2005. Tachyplesin activates the classic complement pathway to kill tumor cells. *Cancer Res.* 65:4614-4622.
- Chen,Y., X.Xu, S.Hong, J.Chen, N.Liu, C.B.Underhill, K.Creswell, and L.Zhang. 2001. RGD-Tachyplesin inhibits tumor growth. *Cancer Res.* 61:2434-2438.

Chernysh,S., S.I.Kim, G.Bekker, V.A.Pleskach, N.A.Filatova, V.B.Anikin, V.G.Platonov, and P.Bulet. 2002. Antiviral and antitumor peptides from insects. *Proc. Natl. Acad. Sci. U. S. A* 99:12628-12632.

Choong,K. and S.Basaria. 2010. Emerging cardiometabolic complications of androgen deprivation therapy. *Aging Male*. 13:1-9.

Cory,S. and J.M.Adams. 1998. Matters of life and death: programmed cell death at Cold Spring Harbor. *Biochim. Biophys. Acta* 1377:R25-R44.

Cruciani,R.A., J.L.Barker, M.Zasloff, H.C.Chen, and O.Colamonici. 1991. Antibiotic magainins exert cytolytic activity against transformed cell lines through channel formation. *Proc. Natl. Acad. Sci. U. S. A* 88:3792-3796.

Daleke,D.L. 2003. Regulation of transbilayer plasma membrane phospholipid asymmetry. *J. Lipid Res*. 44:233-242.

Daleke,D.L. and W.H.Huestis. 1985. Incorporation and translocation of aminophospholipids in human erythrocytes. *Biochemistry* 24:5406-5416.

Dathe,M., J.Meyer, M.Beyermann, B.Maul, C.Hoischen, and M.Bienert. 2002. General aspects of peptide selectivity towards lipid bilayers and cell membranes studied by variation of the structural parameters of amphipathic helical model peptides. *Biochim. Biophys. Acta* 1558:171-186.

De Milito,A. and S.Fais. 2005. Tumor acidity, chemoresistance and proton pump inhibitors. *Future. Oncol*. 1:779-786.

- Dobrzynska,I., B.Szachowicz-Petelska, S.Sulkowski, and Z.Figaszewski. 2005. Changes in electric charge and phospholipids composition in human colorectal cancer cells. *Mol. Cell Biochem.* 276:113-119.
- Domagala,W. and L.G.Koss. 1980. Surface configuration of human tumor cells obtained by fine needle aspiration biopsy. *Scan Electron Microsc.*101-108.
- Drake,C.G. 2010. Immunotherapy for prostate cancer: an emerging treatment modality. *Urol. Clin. North Am.* 37:121-9, Table.
- Dunn,G.P., A.T.Bruce, H.Ikeda, L.J.Old, and R.D.Schreiber. 2002. Cancer immunoediting: from immunosurveillance to tumor escape. *Nat. Immunol.* 3:991-998.
- Edited by Karl Lohner. 2001. Development of Novel Antimicrobial Agents: Emerging Strategies. Horizon Scientific Press.
- Ehrenstein,G. and H.Lecar. 1977. Electrically gated ionic channels in lipid bilayers. *Q. Rev. Biophys.* 10:1-34.
- Eisenberg,D., R.M.Weiss, and T.C.Terwilliger. 1982. The helical hydrophobic moment: a measure of the amphiphilicity of a helix. *Nature* 299:371-374.
- Eliassen,L.T., G.Berge, A.Leknessund, M.Wikman, I.Lindin, C.Lokke, F.Ponthan, J.I.Johnsen, B.Sveinbjornsson, P.Kogner, T.Flaegstad, and O.Rekdal. 2006. The antimicrobial peptide, lactoferricin B, is cytotoxic to neuroblastoma cells in vitro and inhibits xenograft growth in vivo. *Int. J. Cancer* 119:493-500.
- Ellens,H., J.Bentz, and F.C.Szoka. 1985a. H⁺- and Ca²⁺-induced fusion and destabilization of liposomes. *Biochemistry* 24:3099-3106.

Ellens,H., J.Bentz, and F.C.Szoka. 1985b. H⁺- and Ca²⁺-induced fusion and destabilization of liposomes. *Biochemistry* 24:3099-3106.

Engelman,D.M. 2005. Membranes are more mosaic than fluid. *Nature* 438:578-580.

Fadok,V.A., D.R.Voelker, P.A.Campbell, J.J.Cohen, D.L.Bratton, and P.M.Henson. 1992. Exposure of phosphatidylserine on the surface of apoptotic lymphocytes triggers specific recognition and removal by macrophages. *J. Immunol.* 148:2207-2216.

Gatti,L. and F.Zunino. 2005. Overview of tumor cell chemoresistance mechanisms. *Methods Mol. Med.* 111:127-148.

Gofman,Y., S.Linser, A.Rzeszutek, D.Shental-Bechor, S.S.Funari, N.Ben Tal, and R.Willumeit. 2010. Interaction of an antimicrobial peptide with membranes: experiments and simulations with NKCS. *J. Phys. Chem. B* 114:4230-4237.

Hanahan,D. and R.A.Weinberg. 2000. The hallmarks of cancer. *Cell* 100:57-70.

Hancock,R.E. and D.S.Chapple. 1999. Peptide antibiotics. *Antimicrob. Agents Chemother.* 43:1317-1323.

Hancock,R.E. and R.Lehrer. 1998. Cationic peptides: a new source of antibiotics. *Trends Biotechnol.* 16:82-88.

Henzler Wildman,K.A., D.K.Lee, and A.Ramamoorthy. 2003. Mechanism of lipid bilayer disruption by the human antimicrobial peptide, LL-37. *Biochemistry* 42:6545-6558.

Holthuis,J.C. and T.P.Levine. 2005. Lipid traffic: floppy drives and a superhighway. *Nat. Rev. Mol. Cell Biol.* 6:209-220.

- Hoskin,D.W. and A.Ramamoorthy. 2008. Studies on anticancer activities of antimicrobial peptides. *Biochim. Biophys. Acta* 1778:357-375.
- Hristova,K., C.E.Dempsey, and S.H.White. 2001. Structure, location, and lipid perturbations of melittin at the membrane interface. *Biophys. J.* 80:801-811.
- Izadpanah,A. and R.L.Gallo. 2005. Antimicrobial peptides. *J. Am. Acad. Dermatol.* 52:381-390.
- Jacobs,T., H.Bruhn, I.Gaworski, B.Fleischer, and M.Leippe. 2003. NK-lysin and its shortened analog NK-2 exhibit potent activities against *Trypanosoma cruzi*. *Antimicrob. Agents Chemother.* 47:607-613.
- Jaynes,J.M., G.R.Julian, G.W.Jeffers, K.L.White, and F.M.Enright. 1989. In vitro cytotoxic effect of lytic peptides on several transformed mammalian cell lines. *Pept. Res.* 2:157-160.
- Kalyanaraman,B., J.Joseph, S.Kalivendi, S.Wang, E.Konorev, and S.Kotamraju. 2002. Doxorubicin-induced apoptosis: implications in cardiotoxicity. *Mol. Cell Biochem.* 234-235:119-124.
- Kessel,A., D.Shental-Bechor, T.Haliloglu, and N.Ben Tal. 2003. Interactions of hydrophobic peptides with lipid bilayers: Monte Carlo simulations with M2delta. *Biophys. J.* 85:3431-3444.
- Kozłowska,K., J.Nowak, B.Kwiatkowski, and M.Cichorek. 1999. ESR study of plasmatic membrane of the transplantable melanoma cells in relation to their biological properties. *Exp. Toxicol. Pathol.* 51:89-92.
- Lapis,K. 2010. [Host defense peptides and peptidomimetics as new weapons for cancer treatment.]. *Magy. Onkol.* 54:47-58.

Leuschner,C. and W.Hansel. 2004. Membrane disrupting lytic peptides for cancer treatments. *Curr. Pharm. Des* 10:2299-2310.

Lichtenstein,A. 1991. Mechanism of mammalian cell lysis mediated by peptide defensins. Evidence for an initial alteration of the plasma membrane. *J. Clin. Invest* 88:93-100.

Liepinsh,E., M.Andersson, J.M.Ruysschaert, and G.Otting. 1997. Saposin fold revealed by the NMR structure of NK-lysin. *Nat. Struct. Biol.* 4:793-795.

Linser, S. Development of new antimicrobial peptides based on the synthetic peptide NK-2. 2006.

Ref Type: Thesis/Dissertation

Lohner,K. and S.E.Blondelle. 2005. Molecular mechanisms of membrane perturbation by antimicrobial peptides and the use of biophysical studies in the design of novel peptide antibiotics. *Comb. Chem. High Throughput Screen.* 8:241-256.

Lu,Y. 2009. Transcriptionally regulated, prostate-targeted gene therapy for prostate cancer. *Adv. Drug Deliv. Rev.* 61:572-588.

Ludtke,S.J., K.He, W.T.Heller, T.A.Harroun, L.Yang, and H.W.Huang. 1996. Membrane pores induced by magainin. *Biochemistry* 35:13723-13728.

Lyu,P.C., J.C.Sherman, A.Chen, and N.R.Kallenbach. 1991. Alpha-helix stabilization by natural and unnatural amino acids with alkyl side chains. *Proc. Natl. Acad. Sci. U. S. A* 88:5317-5320.

Mader,J.S. and D.W.Hoskin. 2006. Cationic antimicrobial peptides as novel cytotoxic agents for cancer treatment. *Expert. Opin. Investig. Drugs* 15:933-946.

- Mader, J.S., J. Salsman, D.M. Conrad, and D.W. Hoskin. 2005. Bovine lactoferricin selectively induces apoptosis in human leukemia and carcinoma cell lines. *Mol. Cancer Ther.* 4:612-624.
- Mader, J.S., D. Smyth, J. Marshall, and D.W. Hoskin. 2006. Bovine lactoferricin inhibits basic fibroblast growth factor- and vascular endothelial growth factor165-induced angiogenesis by competing for heparin-like binding sites on endothelial cells. *Am. J. Pathol.* 169:1753-1766.
- Mai, J.C., Z. Mi, S.H. Kim, B. Ng, and P.D. Robbins. 2001. A proapoptotic peptide for the treatment of solid tumors. *Cancer Res.* 61:7709-7712.
- Mamdouh, Z., M.C. Giocondi, and C. Le Grimellec. 1998. In situ determination of intracellular membrane physical state heterogeneity in renal epithelial cells using fluorescence ratio microscopy. *Eur. Biophys. J.* 27:341-351.
- Martin, E., T. Ganz, and R.I. Lehrer. 1995a. Defensins and other endogenous peptide antibiotics of vertebrates. *J. Leukoc. Biol.* 58:128-136.
- Martin, S.J., C.P. Reutelingsperger, A.J. McGahon, J.A. Rader, R.C. van Schie, D.M. LaFace, and D.R. Green. 1995b. Early redistribution of plasma membrane phosphatidylserine is a general feature of apoptosis regardless of the initiating stimulus: inhibition by overexpression of Bcl-2 and Abl. *J. Exp. Med.* 182:1545-1556.
- Matsuzaki, K., O. Murase, and K. Miyajima. 1995. Kinetics of pore formation by an antimicrobial peptide, magainin 2, in phospholipid bilayers. *Biochemistry* 34:12553-12559.
- McKeown, S.T., F.T. Lundy, J. Nelson, D. Lockhart, C.R. Irwin, C.G. Cowan, and J.J. Marley. 2006. The cytotoxic effects of human neutrophil peptide-1 (HNP1) and lactoferrin on oral squamous cell carcinoma (OSCC) in vitro. *Oral Oncol.* 42:685-690.

Miteva, M., M. Andersson, A. Karshikoff, and G. Otting. 1999. Molecular electroporation: a unifying concept for the description of membrane pore formation by antibacterial peptides, exemplified with NK-lysin. *FEBS Lett.* 462:155-158.

Mocellin, S., C.R. Rossi, and D. Nitti. 2004. Cancer vaccine development: on the way to break immune tolerance to malignant cells. *Exp. Cell Res.* 299:267-278.

Moran A.L, Scrimgeour K.G, Horton H.R, Ochs R.S, and Rawn J.D. 1994. *Biochemistry*. Prentice Hall.

Munford, R.S., P.O. Sheppard, and P.J. O'Hara. 1995. Saposin-like proteins (SAPLIP) carry out diverse functions on a common backbone structure. *J. Lipid Res.* 36:1653-1663.

Myher, J.J., A. Kuksis, and S. Pind. 1989. Molecular species of glycerophospholipids and sphingomyelins of human erythrocytes: improved method of analysis. *Lipids* 24:396-407.

Naumov, G.N., J.L. Townson, I.C. MacDonald, S.M. Wilson, V.H. Bramwell, A.C. Groom, and A.F. Chambers. 2003. Ineffectiveness of doxorubicin treatment on solitary dormant mammary carcinoma cells or late-developing metastases. *Breast Cancer Res. Treat.* 82:199-206.

Papo, N., A. Braunstein, Z. Eshhar, and Y. Shai. 2004. Suppression of human prostate tumor growth in mice by a cytolytic D-, L-amino Acid Peptide: membrane lysis, increased necrosis, and inhibition of prostate-specific antigen secretion. *Cancer Res.* 64:5779-5786.

Papo, N., D. Seger, A. Makovitzki, V. Kalchenko, Z. Eshhar, H. Degani, and Y. Shai. 2006. Inhibition of tumor growth and elimination of multiple metastases in human prostate and breast xenografts by systemic inoculation of a host defense-like lytic peptide. *Cancer Res.* 66:5371-5378.

- Papo,N., M.Shahar, L.Eisenbach, and Y.Shai. 2003. A novel lytic peptide composed of DL-amino acids selectively kills cancer cells in culture and in mice. *J. Biol. Chem.* 278:21018-21023.
- Papo,N. and Y.Shai. 2003a. Can we predict biological activity of antimicrobial peptides from their interactions with model phospholipid membranes? *Peptides* 24:1693-1703.
- Papo,N. and Y.Shai. 2003b. New lytic peptides based on the D,L-amphipathic helix motif preferentially kill tumor cells compared to normal cells. *Biochemistry* 42:9346-9354.
- Papo,N. and Y.Shai. 2005. Host defense peptides as new weapons in cancer treatment. *Cell Mol. Life Sci.* 62:784-790.
- Pena,S.V., D.A.Hanson, B.A.Carr, T.J.Goralski, and A.M.Krensky. 1997. Processing, subcellular localization, and function of 519 (granulysin), a human late T cell activation molecule with homology to small, lytic, granule proteins. *J. Immunol.* 158:2680-2688.
- Petrey,D., Z.Xiang, C.L.Tang, L.Xie, M.Gimpelev, T.Mitros, C.S.Soto, S.Goldsmith-Fischman, A.Kernytsky, A.Schlessinger, I.Y.Koh, E.Alexov, and B.Honig. 2003. Using multiple structure alignments, fast model building, and energetic analysis in fold recognition and homology modeling. *Proteins* 53 Suppl 6:430-435.
- Pokorny,A. and P.F.Almeida. 2004. Kinetics of dye efflux and lipid flip-flop induced by delta-lysin in phosphatidylcholine vesicles and the mechanism of graded release by amphipathic, alpha-helical peptides. *Biochemistry* 43:8846-8857.
- Powers,J.P. and R.E.Hancock. 2003. The relationship between peptide structure and antibacterial activity. *Peptides* 24:1681-1691.

Robert B.Genis. 1989. Biomembranes Molecular Structure and Function. Springer-Verlag New York Inc..

Saini,S.S., A.K.Chopra, and J.W.Peterson. 1999. Melittin activates endogenous phospholipase D during cytolysis of human monocytic leukemia cells. *Toxicon* 37:1605-1619.

Schaeffer,E.M., S.Loeb, and P.C.Walsh. 2010. The case for open radical prostatectomy. *Urol. Clin. North Am.* 37:49-55, Table.

Schroder-Borm,H., R.Bakalova, and J.Andra. 2005. The NK-lysin derived peptide NK-2 preferentially kills cancer cells with increased surface levels of negatively charged phosphatidylserine. *FEBS Lett.* 579:6128-6134.

Schroder-Borm,H., R.Willumeit, K.Brandenburg, and J.Andra. 2003. Molecular basis for membrane selectivity of NK-2, a potent peptide antibiotic derived from NK-lysin. *Biochim. Biophys. Acta* 1612:164-171.

Schutz,F.A. and W.K.Oh. 2010. Neoadjuvant and adjuvant therapies in prostate cancer. *Urol. Clin. North Am.* 37:97-104, Table.

Schwartz,R.S., Y.Tanaka, I.J.Fidler, D.T.Chiu, B.Lubin, and A.J.Schroit. 1985. Increased adherence of sickled and phosphatidylserine-enriched human erythrocytes to cultured human peripheral blood monocytes. *J. Clin. Invest* 75:1965-1972.

Schweizer,F. 2009. Cationic amphiphilic peptides with cancer-selective toxicity. *Eur. J. Pharmacol.* 625:190-194.

Sebastian Linser. Development of new antimicrobial peptides based on the synthetic peptide NK-2. 2006.

Ref Type: Thesis/Dissertation

Sevcsik,E., G.Pabst, W.Richter, S.Danner, H.Amenitsch, and K.Lohner. 2008. Interaction of LL-37 with model membrane systems of different complexity: influence of the lipid matrix. *Biophys. J.* 94:4688-4699.

Sharma,S.V. 1993. Melittin-induced hyperactivation of phospholipase A2 activity and calcium influx in ras-transformed cells. *Oncogene* 8:939-947.

Shental-Bechor,D., T.Haliloglu, and N.Ben Tal. 2007. Interactions of cationic-hydrophobic peptides with lipid bilayers: a Monte Carlo simulation method. *Biophys. J.* 93:1858-1871.

Shental-Bechor,D., S.Kirca, N.Ben Tal, and T.Haliloglu. 2005. Monte Carlo studies of folding, dynamics, and stability in alpha-helices. *Biophys. J.* 88:2391-2402.

Shin,S.Y., S.H.Lee, S.T.Yang, E.J.Park, D.G.Lee, M.K.Lee, S.H.Eom, W.K.Song, Y.Kim, K.S.Hahm, and J.I.Kim. 2001. Antibacterial, antitumor and hemolytic activities of alpha-helical antibiotic peptide, P18 and its analogs. *J. Pept. Res.* 58:504-514.

Simons,K. and E.Ikonen. 2000. How cells handle cholesterol. *Science* 290:1721-1726.

Singer,S.J. and G.L.Nicolson. 1972. The fluid mosaic model of the structure of cell membranes. *Science* 175:720-731.

Sok,M., M.Sentjurc, and M.Schara. 1999. Membrane fluidity characteristics of human lung cancer. *Cancer Lett.* 139:215-220.

Tossi,A., L.Sandri, and A.Giangaspero. 2000. Amphipathic, alpha-helical antimicrobial peptides. *Biopolymers* 55:4-30.

Udagawa,H. 2009. Chemoradiotherapy: its effectiveness, toxicity, and perspective in the treatment of esophageal cancer. *Ann. Thorac. Cardiovasc. Surg.* 15:359-361.

Utsugi,T., A.J.Schroit, J.Connor, C.D.Bucana, and I.J.Fidler. 1991. Elevated expression of phosphatidylserine in the outer membrane leaflet of human tumor cells and recognition by activated human blood monocytes. *Cancer Res.* 51:3062-3066.

Verkleij,A.J., R.F.Zwaal, B.Roelofsen, P.Comfurius, D.Kastelijn, and L.L.Van Deenen. 1973. The asymmetric distribution of phospholipids in the human red cell membrane. A combined study using phospholipases and freeze-etch electron microscopy. *Biochim. Biophys. Acta* 323:178-193.

Vogel,H., F.Jahnig, V.Hoffmann, and J.Stumpel. 1983. The orientation of melittin in lipid membranes. A polarized infrared spectroscopy study. *Biochim. Biophys. Acta* 733:201-209.

Wang,Z. and G.Wang. 2004. APD: the Antimicrobial Peptide Database. *Nucleic Acids Res.* 32:D590-D592.

White,S.H. and W.C.Wimley. 1998. Hydrophobic interactions of peptides with membrane interfaces. *Biochim. Biophys. Acta* 1376:339-352.

Whitmore,L. and B.A.Wallace. 2004. DICHROWEB, an online server for protein secondary structure analyses from circular dichroism spectroscopic data. *Nucleic Acids Res.* 32:W668-W673.

Whitmore,L. and B.A.Wallace. 2008. Protein secondary structure analyses from circular dichroism spectroscopy: methods and reference databases. *Biopolymers* 89:392-400.

- Wieprecht, T., M. Dathe, E. Krause, M. Beyermann, W. L. Maloy, D. L. MacDonald, and M. Bienert. 1997. Modulation of membrane activity of amphipathic, antibacterial peptides by slight modifications of the hydrophobic moment. *FEBS Lett.* 417:135-140.
- Yang, N., W. Stensen, J. S. Svendsen, and O. Rekdal. 2002. Enhanced antitumor activity and selectivity of lactoferrin-derived peptides. *J. Pept. Res.* 60:187-197.
- Yang, N., M. B. Strom, S. M. Mekonnen, J. S. Svendsen, and O. Rekdal. 2004. The effects of shortening lactoferrin derived peptides against tumour cells, bacteria and normal human cells. *J. Pept. Sci.* 10:37-46.
- Yoon, W. H., H. D. Park, K. Lim, and B. D. Hwang. 1996. Effect of O-glycosylated mucin on invasion and metastasis of HM7 human colon cancer cells. *Biochem. Biophys. Res. Commun.* 222:694-699.
- Zaslhoff, M. 2002. Antimicrobial peptides of multicellular organisms. *Nature* 415:389-395.
- Zelezetsky, I. and A. Tossi. 2006. Alpha-helical antimicrobial peptides--using a sequence template to guide structure-activity relationship studies. *Biochim. Biophys. Acta* 1758:1436-1449.
- Zidovetzki, R., B. Rost, D. L. Armstrong, and I. Pecht. 2003. Transmembrane domains in the functions of Fc receptors. *Biophys. Chem.* 100:555-575.
- Zwaal, R. F. 1978. Membrane and lipid involvement in blood coagulation. *Biochim. Biophys. Acta* 515:163-205.
- Zwaal, R. F., P. Comfurius, and E. M. Bevers. 2004. Scott syndrome, a bleeding disorder caused by defective scrambling of membrane phospholipids. *Biochim. Biophys. Acta* 1636:119-128.

Zwaal,R.F., P.Comfurius, and E.M.Bevers. 2005. Surface exposure of phosphatidylserine in pathological cells. *Cell Mol. Life Sci.* 62:971-988.

Zwaal,R.F., P.Comfurius, and L.L.Van Deenen. 1977. Membrane asymmetry and blood coagulation. *Nature* 268:358-360.

Zweytick,D., G.Pabst, P.M.Abuja, A.Jilek, S.E.Blondelle, J.Andra, R.Jerala, D.Monreal, d.T.Martinez, and K.Lohner. 2006. Influence of N-acylation of a peptide derived from human lactoferricin on membrane selectivity. *Biochim. Biophys. Acta* 1758:1426-1435.

Chapter 5

Curriculum vitae

YASEMIN MANAVBAŞI, MSc



Date of Birth: 16.02.1978
Place of Birth: Ankara
Citizenship: Turkish

Corresponding Addresses:

Private Zinzendorfgasse 18 8010 Graz Austria
Mobile: +43 (0)650 588 08 75
e-mail: yaaseemin@gmail.com

Office Address: Austrian Academy of Sciences
Institute of Biophysics and
Nanosystems Research
Schmiedlstrasse 6
8042 Graz, Austria
Tel: +43 (0)316 4120-321
Fax: +43 (0)316 4120-390
e-mail: yasemin.manavbasi@oeaw.ac.at

Professional Experience

4/2007 – present

Graduate Student

Member of the training network 'Biocontrol' of the Marie Curie Training Program supported by European Union within the 6th Framework Programme
Graz University of Technology, NAWI Doctoral School **Graz, Austria**

PhD Thesis: NKCS peptides as novel anticancer therapeutics

10/2004 – 3/2007

Research Assistant

Gazi University, Faculty of Pharmacology Department of Pharmacology
Ankara, Türkiye

MSc Thesis: The gender differences in the relaxation to levosimendan of human internal mammary artery.

Educational Background

- 2007 – 2010** **PhD**
Graz University of Technology, NAWI Doctorate Program **Graz, Austria**
- 2003 – 2006** **MSc**
Gazi University, Faculty of Pharmacology Department of Pharmacology
Ankara, Türkiye
- 2002 – 2003** **MBA**
Marmara Contemporary Sciences Foundation in collaboration with University
of Maine, Maine Business School **İstanbul, Türkiye**
- 1996 – 2002** **Bachelor Degree**
Orta Doğu Teknik Üniversitesi, Biological Sciences, **Ankara, Türkiye**
- 1993 – 1996** **High School**
Özel Arı Fen Lisesi, **Ankara, Türkiye**